Dynamic system-wide mass spectrometry based metabolomics approach for a new Era in drug research

Castro Perez, J.M.

Part I

LC/MS platform development

Chapter 2

Comprehensive shotgun LC-MS^E lipidomic analysis in osteoarthritis patients

Based on: Castro-Perez J.M., Kamphorst J., DeGroot J., Lafeber F., Goshawk J., Yu K., Shockcor J.P., Vreeken R.J., Hankemeier, T. Comprehensive LC-MS^E lipidomic analysis using a shotgun approach and its application to biomarker detection and identification in osteoarthritis patients. *J Proteome Res* **9**:2377-2389. 2010 (Reprinted with permission)

Part I: Chapter 2

Comprehensive shotgun LC-MS^E lipidomic analysis in osteoarthritis patients

SUMMARY

A fast and robust method for lipid profiling utilizing liquid chromatography coupled with mass spectrometry has been demonstrated and validated for the analysis of human plasma. This method allowed quantifying and identifying lipids in human plasma using parallel alternating low energy and high energy collision spectral acquisition modes. A total of 275 lipids were identified and quantified (as relative concentrations) in both positive and negative ion electrospray ionization mode. The method was validated with five non-endogenous lipids, and the linearity (r^2 better than 0.994), the intra-day and inter-day repeatability (relative standard deviation, 4-6% and 5-8%, respectively) were satisfactory. The developed lipid profiling method was successfully applied for the analysis of plasma from Osteoarthritis (OA) patients. Multivariate statistical analysis by partial least squares-discrimination analysis suggested and altered lipid metabolism associated with osteoarthritis and the release of arachidonic acid from phospholipids.

INTRODUCTION

Lipidomics can be defined as the system-wide characterization of lipids and their interaction with other biochemicals and cells. Lipidomics can be divided into two biochemical areas of equal significance; membrane functional-lipidomics and mediator functional-lipidomics, which pay particular attention to either the exhaustive and quantitative description of membrane lipid components, or the structural identification and quantification of relevant bioactive lipid species. The term "lipidome" can be defined as the comprehensive and non-exhaustive quantitative description of a set of lipid classes which may constitute a cell or bio-organism.

Lipids and their interaction with cells play a crucial role in living organisms (1-3). This is mainly due to the fact that lipids have unique and specific membrane organizing tasks as well as support properties providing cells with distinct sub-cellular membrane compartments. Lipids also extend their functionality levels to other important areas such as their specific and crucial role in cell signaling, endocrine actions and their specific function for energy production and storage. Production of lipids is very extensive by either mammalian or bacterial organisms, and their metabolic pathways are extremely capable of generating a large number of lipid classes typically in the thousands (4) which are functionally and structurally diverse each having a certain biological role. Lipids have a variety of non-polar fatty acid (FA) chains with different backbone structures and different polar head groups. The fatty acid constituents have well-defined structural characteristics, such as *cis*-double bonds in particular positions, which can act as information transporters by selective binding to specific receptors. They can penetrate membranes in their esterified form or be subjected to specific translocation across membranes to carry signals to other cells in different parts of the organism. With regards to lipid storage, such as e.g. triacylglycerols, they are relatively inert until required. In contrast to this, polar lipids have hydrophilic sites that have the capability to bind to membrane proteins and as a consequence influence their dynamics and biological properties. The biological activities of lipids also extend far beyond membranes into e.g., the immune system such as glycolipids with their specific and complex carbohydrate moieties.

Recently, system-wide lipid analysis has attained more interest due to their importance in medical, biological, biotechnological and industrial applications (5-11). Lipids as a whole have shown a direct implication in an important number of human diseases, including cancer and cardiovascular disease. These biological entities are therefore interesting for biomarker discovery. For example, total lipid profiles are measured when trying to assess the efficacy of a certain cholesterol lowering drug such as the 'statins' (12-14) by measuring; triglycerides, cholesterol and high density lipoprotein (HDL)/ low density lipoprotein (LDL) relationships. Profiling of the individual lipids in a system-wide approach is expected to be even more suited to describe an individual's state with regards to health and disease. It is important to understand the classification of lipids in terms of mass spectrometry (MS) as they will have characteristic properties when analyzed by liquid chromatography LC-MS. Therefore, lipids can be catalogued into eight main distinctive classes. Their diversity is mainly based on their fingerprint chemical structure and mainly by the head group of the lipid class: fatty acids, glycerolipids, glycerophospholipids, sphingolipids, sterol lipids, prenol lipids, saccharolipids,

and polyketides (15). For the analysis of lipids in biological samples, LC-MS has played an important role in the detection and identification of lipids. In particular the advent of electrospray has completely transformed the way in which these compound classes are characterized and quantified with extreme sensitivity in the low femtogram levels. Electrospray is a soft ionization technique and in the vast majority of cases will generate protonated or deprotonated molecules depending on the polarity of the ionization mode utilized. In addition to this, it is not uncommon to generate molecular adducts provided by cations such as Na^+, K^+, or NH_4^+ in positive ion mode. These adducts mainly originate from the specific mobile phase used for the analysis. On the other hand, chromatography has also further evolved with, e.g., developments in the fabrication of small particle sizes such as in the sub 2µm range to obtain chromatographic separations in a much shorter analytical run without the loss of specificity and chromatographic fidelity. This so-called ultra performance LC (UPLC) (16-19) is now widely used and applied to not only lipid analysis but also other areas such as pharmaceutical, metabolomic, proteomic, biopharmaceutical and chemical analyses. There are several strategies which are widely used for the separation of lipids prior to introduction in the mass spectrometer. Normal phase LC-MS separates phospholipids into their respective classes. The separation is important as a means of classification because the separation is attained based on their respective polar head groups with complete disregard of their *sn*-1 and *sn*-2 fatty acid substituents. This is not an uncommon approach to lipid analysis by LC-MS and suitable MS 'friendly' solvents have been used to achieve such separations. In contrast to normal phase separations for lipid analysis reverse phase (RP) separations have the signature characteristic of cataloguing the lipids according to the overall polarity and the fatty acid composition in the *sn*-1, *sn*-2 and *sn-3* locations. Such a RP separation is more or less orthogonal to normal phase. The ideal situation would be the use of two-dimensional LC in which normal and reversed phases are comprehensively coupled, but such a coupling is not straightforward, and was not the aim of the current project. In terms of mass spectrometric analyzers, lipid analysis has been developed and implemented successfully with tandem quadrupoles and linear ion traps (21-26). In addition there are other mass analyzers, like orbitraps, fourier transform ion cyclotron resonance (FTICR) and hybrid quadrupole orthogonal time-of-flight technology (Q-Tof), which may be utilized for the analysis of phospholipids. It is important for these studies that the mass analyzer of choice can provide exact mass information as this will help to determine the elemental composition of the lipid of interest. The Q-ToF (27) provides such mass measurement and is designed as follows; the first quadrupole focuses all ions (in RF –only mode) or selected ions into the second quadrupole, which acts as a collision cell. Ions entering this collision cell will either be fragmented by collision induced dissociation (CID) or will be transferred without fragmentation into the time of flight region for subsequent detection. Technological advances have made hybrid mass spectrometers such as the Q-ToF superior over more conventional tandem quadrupole or linear ion trap with regards to enhanced mass accuracy and spectral resolution next to sensitivity in full scan mode. A clear example of this is the ability of the Q-ToF to conduct many precursor and neutral loss acquisitions over a single experimental run using an instrument acquisition mode called MS^E (28-30). This overcomes duty cycle issues associated with other scanning instruments with a high number of precursor or neutral loss ions per single injection. Furthermore, during an MS^E acquisition exact mass information is obtained, which is used to remove false positives. In this paper, a rapid and simple

reversed phased UPLC/ TOF MS^E strategy to detect and identify multiple classes of lipids in extracted human plasma will be demonstrated. The methodology is applied to the study of osteoarthritis in humans.

MATERIALS AND METHODS

Chemicals

Mass spectrometry grade isopropanol, acetonitrile and ammonium formate (AmmFm 99.995%) were purchased from Sigma (St. Louis, MO). Water was obtained from a Millipore high purity water dispenser (Billerica, MA). Dichloromethane and methanol were obtained from Thermo Fisher Scientific (New Jersey, NJ) The mobile phase for this study was prepared as follows; solvent A was prepared by adding 400 mL of H_2O to 600mL of acetonitrile followed by the addition of 0.6306 ± 0.1 g of AmmFm to yield a 10mM total concentration of AmmFm. For solvent B, 100 mL of acetonitrile was added to 900 mL of isopropanol followed by the addition of 0.6306 ± 0.01 g of AmmFm to yield a 10 mM total concentration of AmmFm. Prior to use, both solvents A and B were degassed in an ultrasonic bath for 30 minutes. Lipid standards of 1-heptadecanoyl-2-hydroxy-*sn*-glycero-3-phosphocholine LPC (17:0/0:0), 1-nonadecanoyl-2-hydroxy-*sn*-glycero-3-phosphocholine LPC (19:0/0:0), 1,2-dipentadecanoyl-*sn*-glycero-3-phosphoethanolamine PE (15:0/15:0), 1,2-diheptadecanoyl-*sn*-glycero-3-phosphoethanolamine PE (17:0/17:0), 1,2-dimyristoyl- *sn*-glycero-3-[phospho-rac-(1-glycerol)] (sodium salt) PG (14:0/14:0), 1,2-diheptadecanoyl*sn*-glycero-3-[phospho-rac-(1-glycerol)] (sodium salt) PG (17:0/17:0), 1,2-diheptadecanoyl-*sn*-glycero-3-phosphocholine PC (17:0/17:0) and 1,2-dinonadecanoyl-*sn*-glycero-3-phosphocholine PC (19:0/19:0) were purchased from Avanti Polar Lipids (Alabaster, AL, USA). 1,2,3-Tripentadecanoylglycerol TG (15:0/15:0/15:0), 1,2,3-triheptadecanoylglycerol TG (17:0/ 17:0/17:0) were obtained from Sigma (Zwijndrecht, The Netherlands). Leucine enkephalin (Sigma, St. Louis, MO, USA) was used as the lockmass solution at a concentration of 1 ng/µL in a solution of acetonitrile/water +0.1% Formic acid (50/50 v/v).

Lipid nomenclature

Throughout the entire paper and in order to follow a common standard lipid language, the lipid nomenclature described by LIPIMAPS (http://www.lipidmaps.org) was followed.

Lipid preparation and extraction

Lipid extracts from human plasma were prepared according to the protocol described by Hu (35). Human plasma samples were prepared and extracted in a biosafety level 2 (BL2) fume hood. The reproducibility and efficacy of the methodology was tested with a set of human plasma extracts over the total procedure. The validation extracts were prepared by spiking 5 different non-endogenous lipids (LPC 19:0/0:0, PG 14:0/14:0, PE 15:0/15:0, PC 19:0/19:0 and TG 15:0/15:0/15:0) and their corresponding internal standards into pooled healthy human plasma. The concentration ranges for each of the non-endogenous lipids and their internal standards were; LPC 19:0/0:0 0, 1.25, 2.5, 5, 20, 80, 160 µg/mL and the internal

standard LPC 17:0/0:0 were used at a final concentration of 15µg/ml; PG 14:0/14:0 0, 5, 10, 20, 80, 320 □g/mL and the internal standard PG 17:0/17:0 were used at a final concentration of 20µg/ml ; PE 15:0/15:0 0, 2.5, 5, 10, 40, 160, 320 µg/mL and the internal standard PE 17:0/17:0 were used at a final concentration of 20 µg/ml; PC 19:0/19:0 0, 3.75, 7.5, 15, 60, 240, 480µg/mL and the internal standard PC 17:0/17:0 were used at a final concentration of 40 µg/ml; TG 15:0/15:0/15:0 0, 1.25, 2.5, 5, 20, 80,160µg/mL and the internal standard TG 17:0/17:0/17:0 were used at a final concentration of 25µg/ml. Each calibration standard was injected in triplicate. The lipid fraction was extracted using a simple liquid-liquid extraction (LLE) methodology in which 30 µL of human plasma was mixed with a dichloromethane (DCM) /methanol mixture (31) (2:1,v/v) in accordance with the method described by Bligh and Dyer (31).

The method was validated by spiking the samples before and after preparation as follows; before the sample preparation; 30 µL of IS and 30 µL of the validation calibration mixture were added to 30µL of human plasma sample followed by the addition of 180 µL of MeOH and 360 µL of DCM. A total of 340 µL of lipid extract from the lower organic phase was collected and then 60 µL of 2:1 DCM/MeOH was added. This mixture was diluted 5 times with injection solvent; 10 µL was injected into the LC-MS system

The procedure for spiking after the sample preparation was the same as that described for spiking before except the order in which the 60 µL of 2:1 DCM/MeOH and 30µL of IS plus 30 µL of validation standard mixture was added. For the blank sample, 30 µL of human plasma was replaced by 30 µL of HPLC-MS grade water and the 60 µL of the two sets of standard mixtures were replaced by 60 µL of 2:1 DCM/ MeOH.

Osteoarthritis sample analysis

Heparinized plasma samples were collected from 59 subjects (all female donors) that were part of the Dutch CHeCK cohort (31). Permission was granted to analyze the samples for the purpose of this particular study. Subjects were classified based on radiologic features of osteoarthritis in knee and hip joints (Kellgren-Lawrence Grading). The KL-grade (0-4) was determined for each joint and a summed osteoarthritis load was calculated for each subject by summing the KL grade of the individual joints, resulting in a theoretical range from 0 (no OA in knees of hips) to 16 (severe OA in all joints). Since the CHeCK cohort comprised subjects with mild OA, the actual range in the current 59 subjects was 0 to 8. The samples were analyzed by LC-MS individually, each sample group contained the following number of subjects ; group 0 (n =26) , group 1 (n = 6), group 2 (n = 8), group 3 (n = 4), group 4 (n = 8) , group 5 (n =1), group 6 (n = 2), group 7 (n = 2), group 8 (n = 2). For the purpose of the statistical analysis the samples were classified under the following groups; Control subjects with a total OA score of 0 (no OA in knees of hips); Early OA subjects with a total OA score of 1-3 and Moderate OA, subjects with a total OA score of 4-8. All patients had similar body mass index (BMI).

UPLC analysis

An Acquity UPLC (Waters, Milford, MA, USA) was used for the inlet. Human plasma extracts were injected onto a 1.8 µm particle 100 x 2.1 mm id Waters Acquity HSS T3 column (Waters, Milford, MA, USA) which was heated to 55 °C in the column oven. The average column pressure was ca. 10,000 psi. A binary gradient system consisting of acetonitrile and water with 10 mM ammonium formate (60:40, v/v) was used as eluent A. As for eluent B, it consisted of acetonitrile and isopropanol both containing 10mM ammonium formate (10:90, v/v). The sample analysis was performed by using a linear gradient (curve 6) over a 15 minute total run time; during the initial portion of the gradient, it was held at 60% A and 40% B. For the next 10 minutes the gradient was ramped in a linear fashion to 100% B and held at this composition for 2 minutes hereafter the system was switched back to 60% B and 40% A and equilibrated for an additional 3 minutes. The flow rate used for these experiments was 0.4mL/min and the injection volume was 10 µL.

Mass Spectrometry

The inlet (UPLC system) was coupled to a hybrid quadrupole orthogonal time of flight mass spectrometer (SYNAPT HDMS, Waters, MS Technologies, Manchester, and UK). Electrospray positive and negative ionization modes were used. A capillary voltage and cone voltage of ±3 kV and ±35 V respectively were used for both polarities. The desolvation source conditions were as follows; for the desolvation gas 700 L/hr was used and the desolvation temperature was kept at 400^{o}C. Data acquisition took place over the mass range of 50-1200 Da for both MS and MS^{E} modes. The system was equipped with an integral LockSpray unit with its own reference sprayer that was controlled automatically by the acquisition software to collect a reference scan every 10 seconds lasting 0.3 seconds. The LockSpray internal reference used for these experiments was Leucine enkephalin. The reference internal calibrant was introduced into the lock mass sprayer at a constant flow rate of 50 µL/min using an external pump. A single lock mass calibration at m/z 556.2771 in positive ion mode and m/z 554.2615 in negative ion mode was used for the complete analysis. The mass spectrometer was operated in the MS^{E} mode of acquisition for both polarities. During this acquisition method, the first quadrupole Q1 is operated in a wide band RF mode only, allowing all ions to enter the T-wave collision cell. Two discrete and independent interleaved acquisitions functions are automatically created. The first function, typically set at 5 eV, collects low energy or unfragmented data while the second function collects high energy or fragmented data typically set by using a collision energy ramp from 20-30 eV. In both instances, Argon gas is used for CID. The advantage of this acquisition mode lies in the fact that it is an unbiased strategy to collect both unfragmented and fragmented ions which consecutively can be used for e.g. quantification and fragment-ion information, without prior knowledge of the sample composition. The latter experiment can be considered to be a product-ion scan, a pre-cursor ion- or neutral-loss “like” scan. This technique was able to produce a more generic, simple, fast and yet elegant profiling approach to complex lipidomic samples. Applying

this technology allowed the specific detection of intact $[M+H]^+$ or $[M-H]^-$ ions, precursor- and neutral loss-like ions in either positive or negative ionization mode upon collision-induced dissociation.

The specificity and reliability of this methodology allowed us to use this technology as a 'shotgun' LC-MS approach to search for fatty acids (FA), cholesteryl esters (ChoE), phospholipids (PL), monoacyglycerides (MG), diacylglycerides (DG) and triacylycerides (TG) in an unbiased and reliable manner. For instance, in positive ion mode PCs and SMs are readily detected as protonated molecules or cations. Upon CID they both generate the m/z 184.0739 fragment-ion corresponding to the polar hear group, $[(CH_3)_3N^+C_2H_4OP\ (OH)_2\ O]$. Ions yielding structural information are of low abundance and typically other solvents/modifiers such as LiOH are added either in the mobile phase or post-column (32) to obtain information on the FA chain length and number of carbon atoms**.** As a matter of interest, the fragmentation pathway for the generation of this particular fragment-ion (m/z 184.0739) has been extensively studied which indicates direct involvement of a α-hydrogen mainly of the fatty acyl chain at *sn*-2 (33).

Data Processing

For the determination of the repeatability, linearity and recovery, the ratio of the peak areas of the endogenous lipid and the corresponding internal standard was calculated. The internal standard for the lipids LPC 19:0/0:0, PG 14:0/14:0, PE 15:0/15:0, PC 19:0/19:0 and TG 15:0/15:0/15:0 were LPC 17:0/0:0, PG 17:0/17:0, PE 17:0/17:0, PC 17:0/17:0 and TG 17:0/17:0/17:0, respectively.

A quantitative and qualitative software tool called TargetLynx (Waters MS Technologies, Manchester, UK) was utilized for the determination of the peak areas of calibration analytes and internal standards followed by the generation of calibration lines. In addition to this, the above mentioned software algorithm was also capable of generating a peak list (m/z, retention time, peak area, mass accuracy) containing a pre-defined list of lipids, from which the raw data was mined verifying the presence or absence of these biochemicals. A master list was generated in a .txt format and was used for further evaluation.

For the MS^E data processing, the software tool MetaboLynx XS (Waters MS Technologies) was utilized to align the low energy information with the high energy information. Typically this tool is utilized for processing xenobiotics but it is equally applicable to this concept. This algorithm allowed for the search of common precursor ions, diagnostic precursor ions and neutral losses from the high energy data and by parallel alignment with the low energy data and thus locating the unfragmented molecule.

In the case of the osteoarthritis sample analysis, MarkerLynxXS (Waters MS Technologies) was used as the primary tool for data deconvolution and multivariate statistical analysis. The data set was normalized to the total number of peaks identified as variables (exact mass-retention time pairs (EMRT) and peak intensities) and pareto scaling was utilized for

the multivariate statistical analysis. For the database search, lipidmaps *on-line* searching tools (http://www.lipidmaps.org) was used.

RESULTS AND DISCUSSION

UPLC-TOF MS^E Analysis

In order to understand the lipidome and the biological implications it is important to be able to catalogue and quantify lipids into their respective molecular classes. The use of UPLC enabled a fast sample turn around in a total time of 15 minutes which is suitable for a rapid profiling screening strategy. This is about 3x faster than it would take for a similar HPLC method under the same conditions (34). Figure 1 highlights the retention time windows of the lipid classes in the UPLC/TOF MS chromatogram in positive and negative ion mode. In other words, these are region-specific chromatographic areas where we could focus our attention when searching for certain lipid classes or for specific fraction collection experiments.

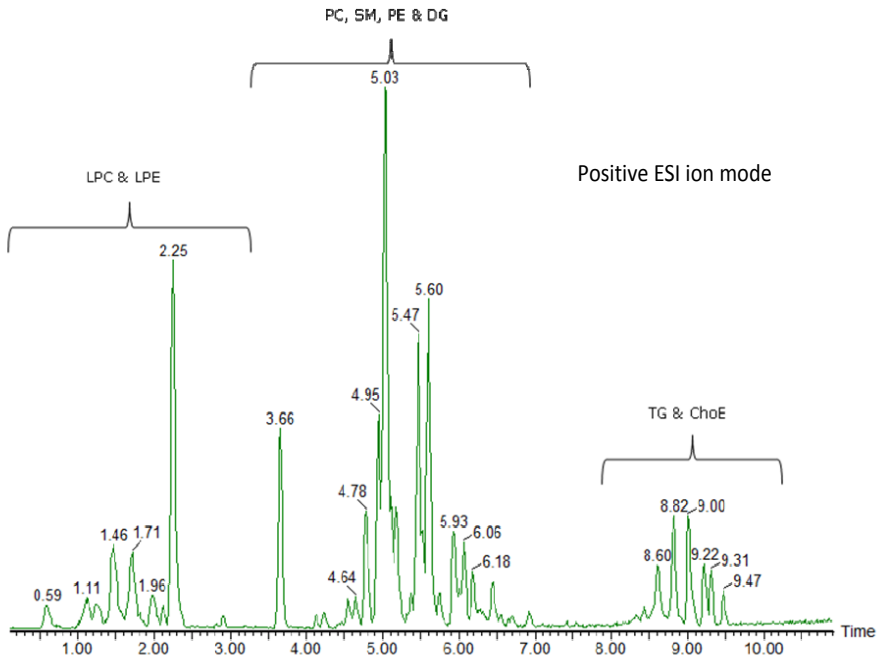

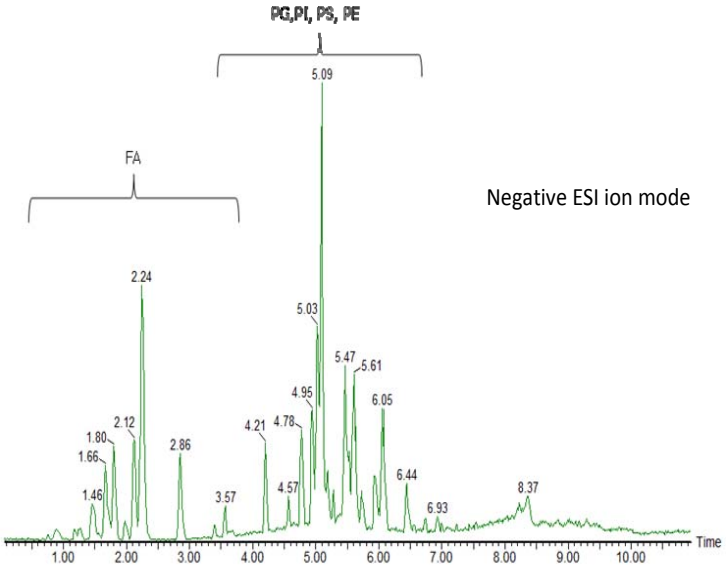

Figure 1. Base peak UPLC/TOFMS chromatogram of a human plasma extract using electrospray ionization in positive and negative mode; different lipid classes elute in different elution time windows. For the experimental details see Materials and Methods.

Abbreviations: ChoE= cholesterol ester; PC = phosphatidylcholine; FA = free fatty acid; TG = triglyceride; DG = diacylglyceride; PS = phosphatidylserine; PI = phosphatidylinositol; PG = phosphatidylglycerol; PE = phosphatidylethanolamine; LPE = Lyso phosphatidylserine; LPC = Lyso phosphatidylcholine; SM= sphingomyelin.

Linearity

For the developed RP-UPLC-TOFMS^E method, five different non-endogenous lipids were spiked to 30 µL of human plasma at six different concentrations (C0-C6), where the calibration ranges were different for the five non-endogenous lipids (Table 1). For each of the five lipids a calibration line was generated using the ratios of the non-endogenous lipid peak areas and their corresponding internal standard (IS). Different polarity ionization modes were used for the different lipids, due to the difference in the preferential ionizations for the different polar head groups. They were divided in the following order for all the validation experiments; positive ion electrospray mode (LPC 19:0/0:0, PC 19:0/19:0 and TG 15:0/15:0/15:0) and negative ion electrospray mode (PG 14:0/14:0 and PE 15:0/15:0). The linear regression r^2 was better than 0.994 for all five non endogenous lipid species (Table 1). These results are comparable to those published by Laaksonen and Hu (35, 36). In order to prove the robustness of the methodology described in this paper, good linearity was also obtained when PC 17:0/17:0 was used as the internal standard for LPC 19:0/0:0 (r^2, 0.995) and for TG 15:0/15:0/15:0 (r^2, 0.996) in electrospray positive ion mode. A good correlation was obtained in electrospray negative ion

mode when PE 15:0/15:0 was used as the internal standard for PG 14:0/14:0 (r2, 0.998). In all these cases also the RSDs were acceptable (data not shown).

Table 1. Validation results of non-endogenous validation standards; response determined as ratio of response of validation standard and corresponding internal standard; 5 non-endogenous lipids and internal standards were spiked to human plasma prior to sample preparation. Each calibration point was injected in triplicate.

Validation Standards/IS Results										
	LPC (19:0/0:0)/ LPC (17:0/0:0)		PC (19:0/19:0)/ PC (17:0/17:0)		PE (15:0/15:0)/ PE (17:0/17:0)		PG (14:0/14:0)/PG (17:0/17:0)		TG (15:0/15:0/15:0)/TG (17:0/17:0/17:0)	
conc. Level	conc (µg/mL)	Average RSD (%)	conc (µg/mL)	Average RSD (%)	conc (µg/mL)	Average RSD (%)	conc (µg/mL)	Average RSD (%)	conc (µg/mL)	Average RSD (%)
C1	1.25	-4.6	3.75	-7.7	2.5	-9.0	5	-7.2	1.25	1.0
C2	2.5	-6.1	7.5	-0.4	5	-0.1	10	8.3	2.5	-1.2
C3	5	-2.8	15	15.9	10	1.8	20	12.1	5	9.2
C4	20	-6.1	60	1.0	40	5.7	80	7.9	20	-7.1
C5	80	0.4	240	1.8	160	-0.2	320	-4.0	80	4.7
C6	160	0.8	480	-1.3	320	-0.7			160.0	-0.8
slope	0.0477		0.0164		0.0142		0.0067		0.0226	
intercept	-0.0117		0.0128		0.0184		0.0173		0.0064	
R^2	0.9993		0.9993		0.999		0.9943		0.9982	

Reproducibility

The intra-day and inter-day variation was assessed by performing repeated sample preparations and analysis during three consecutive days; this consisted of sample preparation, extraction and analysis in triplicates. One human plasma sample was divided into several aliquots stored at -20^{o}C for each sample preparation step. Quality controls for each of the 5 non-endogenous lipid standards were prepared in plasma at the following concentration levels; LPC 19:0/0:0 (20µg/mL), PG 14:0/14:0 (80µg/mL), PE 15:0/15:0 (40µg/mL), PC 19:0/19:0 (60µg/mL) and TG 15:0/15:0/15:0 (20µg/mL). The intra-day and inter-day variation were calculated as the mean ratios of the peak area of the selected lipid with the corresponding IS spiked to human plasma (Supplemental information Figure S1). The RSD for the intra-day variation for all the 5 non-endogenous lipids ranged from 4.3-6.2%. For the inter-day variation, the RSD for all the non-endogenous lipids ranged from 4.8-8%.

Recovery

In the recovery section of the validation, the same 5 non-endogenous lipids with their respective internal standards already cited in the method were used. These lipids were spiked before and after extraction. Each plasma and pretreated sample was prepared in triplicate in 3 consecutive days, and analyzed in triplicate. The recovery for each non-endogenous lipid in the validation set was calculated as the ratio of the peak area for the particular lipid in the sample prior to extraction and in the samples spiked after extraction. The recoveries were calculated at the following concentration levels for all the lipids in the validation set; LPC 19:0/0:0 (20µg/mL), PG 14:0/14:0 (80µg/mL), PE 15:0/15:0 (40µg/mL), PC 19:0/19:0

(60µg/mL) and TG 15:0/15:0/15:0 (20µg/mL). The average recoveries over the 3 day recovery test (Supplemental information Figure S2) were 74% for the LPC 19:0/0:0, 94% for the PC 19:0/19:0, 81% for the PE 15:0/15:0, 79% for the PG 14:0/14:0 and 82% for the TG 15:0/15:0/15:0. The recoveries were considered to be acceptable for routine lipid profiling experiments.

Lipid Identification and MS^E

With respect to the lipid identification step, it was possible to identify 275 major fatty acids lipids and TG's (Table S1 in the supplemental information) in these human plasma samples. It is worth pointing out that in total more than 1500 peaks were detected but it was beyond the scope of this paper to identify each one of all entries and we only focused on the most abundant lipid species. This methodology and in particular the use of the highly efficient LC separation allowed for the separation of isomers of several lipids.

These 275 human fatty acids, lipids and TG's are classified according their respective groups, TGs (77), PC (65), SM (43), PS (31), LPC (22), FA (14), PI (7), ChoE (6), PE (4), PG (3), LPE (2) and DG (1). By observing this table closely (Table S1 in the supplemental information section) it is obvious that the top 10 most abundant ions (Table S2 in the supplemental information) belong to the PC, SM and TG lipid class. The most abundant phospholipid was a PC with an absolute peak area of 311 at a retention time of 5.02 minutes. At this particular retention time a protonated molecule $[M+H]^+$ with an m/z of 758.5718 corresponding to the elemental composition $C_{42}H_{80}NO_8P$ (error of +2.4 ppm) was assigned to a PC compound with a 1-acyl 34:2 moiety. The most abundant peak of the second most abundant phospholipid class found in the top 10 entries had a retention time of 4.78 minutes and a peak area of 60. The corresponding spectrum shows a protonated molecule $[M+H]^+$ at m/z 703.5767 and an elemental composition of $C_{39}H_{79}N_2O_6P$ with an error of +1.9 ppm. This phospholipid was assigned as the 2-amido 16:0 of the SM class. The most abundant peak of the third most abundant lipid class (retention time 8.82 minutes and m/z 874.7885 for the $[M+NH_4]^+$ ion) was assigned to the triacylglyceride (TG) 1-acyl 52:3 ($C_{55}H_{103}NO_6$ +2.5 ppm).

One approach which can be used to obtain MS^2 information is to carry out data-dependent experiments (37). During data-dependent experiments it is possible to collect MS and MS^2 data in a serial process, that is when a specific ion of interest is detected in full scan mode and after a specific set of criteria, e.g. peak intensity, retention time, inclusion- and/or exclusion criteria, are met, the mass spectrometer will switch to MS^2 mode and collect fragment-ion data. However, during these experiments for complex samples co-elution of multiple lipids, at low and high level concentrations will occur, and the data-dependent fragmentation experiments may vary from sample to sample. A 'good' data-dependent method relies heavily on the fact that the scientist has previous knowledge of the type of biochemicals which are expected to be detected, the method itself including m/z ranges and ion intensity thresholds which need to be set accordingly in order to prevent inclusion of false positives, therefore adding complexity to the experiment. As a result, for the qualitative

analysis lipids may be missed, and quantitative analysis is not possible with data-dependent MS/MS data. Also, if the MS/MS experiments are too slow, not enough full scan MS experiments are carried out for quantitative analysis. In this context the acquisition rate of the mass spectrometer and the speed of the chromatography are important factors to be considered.

In contrast, during the MS^E approach all ions generated in the ion source enter the collision cell, and alternating a (i) low energy collision experiment is carried out resulting in only very modest or no fragmentation and a (ii) higher energy collision experiment is carried out resulting in fragment ions; in both cases all product ions are acquired in the TOF MS detector. The use of MS^E data results in multiple levels of information which is extremely useful when trying to confirm the identity of a specific compound. For example, one could focus on determining the polar head group or the carbon length of the FA moiety. With this data independent acquisition mode it is possible to perform an *ad-hoc de-novo* profiling type of experiment. These experiments capture a myriad of information which may be used to data mine complex data sets by extracting accurate mass full scan chromatograms or accurate mass high energy chromatograms which may contain key diagnostic fragment-ions. Since we now have both low and high energy information within the same data file, it is possible to obtain accurate mass, fragment-ion, precursor ion and neutral loss 'like' data to search for diagnostic ions or common neutral losses.

Therefore, the specificity arising from the accurate mass precursor 'like' ion scanning allowed for an extended application of this technique not just for a single diagnostic fragment-ion but for a large number of them without the loss in performance as seen when the same experiment is performed with a tandem quadrupole or linear ion trap. In addition to this, a higher level of specificity is obtained because the use of accurate mass and a high level of mass spectral resolution in both the low and the high energy modes. To illustrate this powerful approach, Figure 2 highlights the possibility to extract an accurate mass ion chromatogram with a narrow mass window of 30mDa for the phosphatidylcholine head group. By alignment of the low energy data with the high energy data, which is carried out automatically with the software (MetaboLynx XS), all low energy corresponding entries which have this product ion of interest will be reported. From this figure it is clearly visible that not only the phosphatidylcholine fragment-ion at m/z 184.0731 was very abundant, but also selectively allowed the search for the LPC, PC and SM phospholipid classes. Of course this is notwithstanding the fact that all other important full scan and fragment-ion information belonging to other lipid classes are acquired within the single LC-MS^E analysis and can be data mined at any time. This approach is totally unbiased and as such it is possible to search for other diagnostic fragments as 'all fragment-ions' should be accounted for. This will allow for the identification of high and low abundance species in a relatively simple manner. However, having said this, the data generated here is very complex and even though it is possible to obtain a 'quick look and see' of what is there in a manual fashion. Ultimately, powerful software algorithms in the MS^E software allows for correlation and alignment between low and high energy data

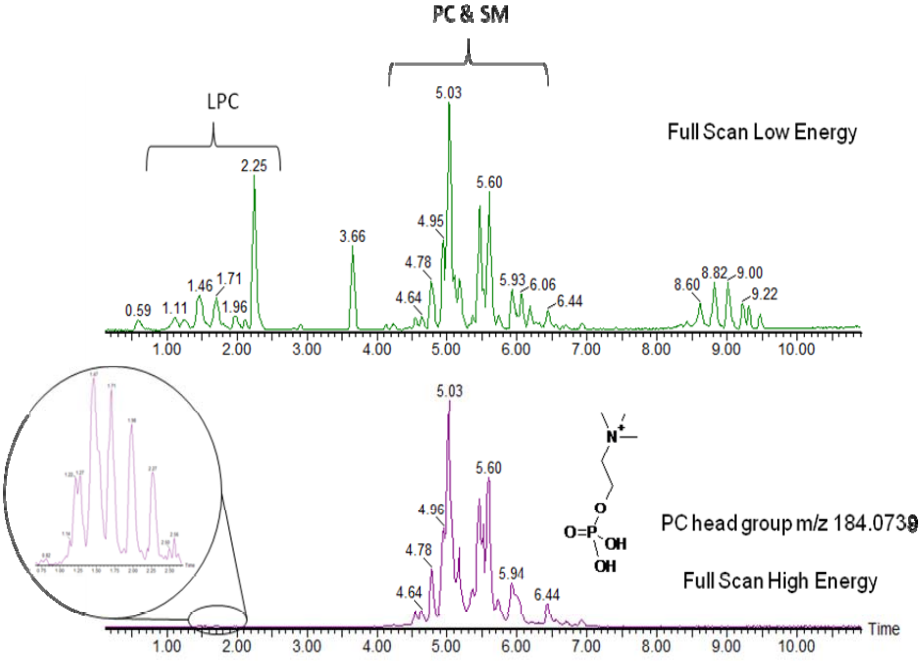

Figure 2. Low-(top) and high-(bottom) collision energy full scan MS chromatogram obtained by MS^E approach using conditions as described in Methods and Materials. It can be clearly seen that the fragment-ion for the phosphocholine head group m/z 184.0739, being characteristic for LPC, PC and SM can clearly be used for identification of individual lipids within one class followed by alignment with the low energy trace.

The high energy data is produced by CID, which in turns gives rise to an extensive number of fragment-ions. If, for instance we take the diagnostic fragment-ion of the phosphatidylcholine species at m/z 184.0733 (error, -3.3 ppm) (Figure 3 section B) it can be observed how the low energy (Figure 3 section A) gives rise to the ion at m/z 758.5697 (-0.5 ppm) $[M+H]^+$ (PC 16:0/18:2). The corresponding fragments of this ion are visible in the high energy spectrum. The ion with the highest abundance is clearly the diagnostic fragment-ion for the PC's of m/z 184.0733 corresponding to the polar head group. However, next to this ion several other fragment-ions are present in the high energy spectrum at a much lower abundance. Further examination of these fragment-ions show that they can be associated with the FA chains of the molecule. Without the use of lithiated adducts, the ion at m/z 184.0733 is the only high abundance ion which dominates the spectrum and hardly any *sn-1* or *sn-2* information as to the assignment for the identities and position of the FA substituent is obtained. Having said that, it is still possible to generate information detailing fatty acid branching information in a chromatographic timeframe. As shown in figure 3 section A of the spectra reveals the low energy information containing the unfragmented PC (16:0/18:2) and section B contains fragment-ion information detailing the

loss of the polar head group at m/z 184.0733 and the cleavages of the *sn-2* m/z 496.3410 and *sn-1* m/z 520.3407, subsequent H_2O losses from the sn-2 m/z 478.3300 and sn-1 m/z 502.3315 were also detected. Therefore, helping to decipher the lipid polar head and FA composition.

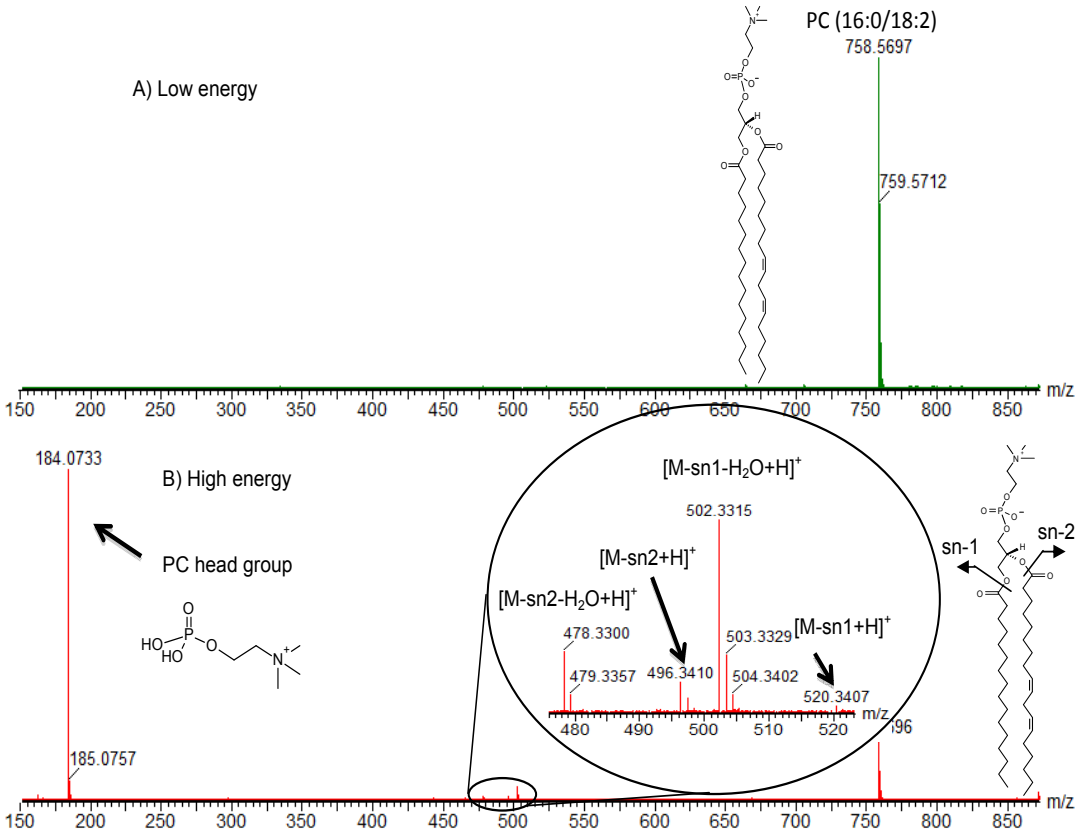

Figure 3. Low- (top) and high- (bottom) collision energy exact mass spectra of PC (16:0/18:2). The low energy spectrum only contains the pre-cursor ion at m/z 758.5697 whereas in the high energy spectrum various diagnostic fragments appear as the loss of the various FA chains at 496.3410 and 520.3407 and their respective water losses. Next also the major fragment ion at m/z 184.0733 can be seen corresponding to the polar head group.

PC can also be presented as plasmanyl-phosphocholines and plasmenyl-phosphocholines (38). These plasmanyl- and plasmenyl- phosphatidylcholine species mainly yield upon MS/MS the fragment-ion at m/z 184.0739, (being the phosphatidylcholine head group) , such as the diacyl-phosphocholines. Sphingomyelins also share the same phosphocholine diagnostic fragment-ion as with the PC. The only difference from the PC is in the fact that they are linked to the phosphocholine polar head group by an *N-acyl* FA linked to a long-chain hydrocarbon. Another example of the

benefit of applying MS^E acquisition and subsequently obtaining more detailed information on *sn-1* and *sn-2* Acyl FA chain length is shown in Figure 4. Here the low energy ion trace of m/z 782.5694 corresponding to PC 36:4, i.e. representing several possible isomers as well as the high energy traces of m/z 502.3292 and m/z 478.3292 are shown (Figure 4B and 4C, respectively). It is possible to see very good alignment between the peak at 4.65 minutes in the low energy scan and the peak with the same retention time (only difference is the inter-scan delay which is consistent throughout the experiment) in the high energy trace for m/z 502.3292. This product ion can be assigned as $[(M\text{-}sn\text{-}1\text{-}H_2O)+H]^+$ or $[(M\text{-}sn\text{-}2\text{-}H_2O)+H]^+$ corresponding to either the *sn-1* or *sn-2* acyl FA loss of PC 18:2/18:2. The two low energy peaks in the m/z 782.5694 trace at retention times 4.95 minutes and 5.45 minutes both have corresponding aligned peaks by retention time belonging m/z 478.3292 which is a descriptive ion for $[(M\text{-}sn\text{-}1\text{-}H_2O)+H]^+$ or $[(M\text{-}sn\text{-}2\text{-}H_2O)+H]^+$ to either the *sn-1* or *sn-2* acyl FA for PC 16:0/20:4 or PC 20:4/16:0). The other peaks in figure 4B and C correspond to the remaining acyl FA fragments for other lipids which had in common the masses of m/z 478.3292 and m/z 502.3292. From this data, vital information is acquired which gives insight to the FA composition.

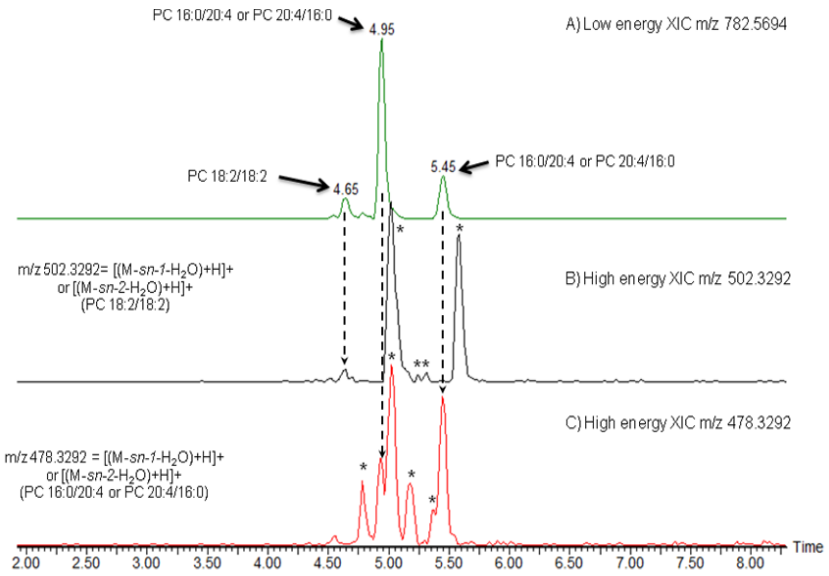

Figure 4. (A) Shows the low energy trace for PC 36:4 (m/z 782.5694) and the high energy traces for (B) m/z 502.3292 and (C) m/z 478.3292 highlighting the corresponding fragment-ions (dashed lines) of the various structures for PC (36:4) providing information on their possible FA composition.

*Acyl FA corresponding to other lipids

Due to its generic nature, this method is not only specific to phospholipids but any other biochemical entity present in the sample, for example TGs and ChoE's detected in electrospray positive ion.

The fragment-ions of TG's (39) have been comprehensively characterized by Murphy *et al* and as in the case of phospholipids it gives rise to diagnostic fragment-ions and neutral losses which may be used to determine the length and composition of the FA chains. It has to be noted that the protonated molecules obtained by the described method are in the form of the ammonium adduct $[M+NH_4]^+$. Under CID reactions in the collision cell, the decomposition of the $[M+NH_4]^+$ ion results in the neutral-loss of i) NH_3 and ii) the acyl-side chains, to generate the diacyl product ion. MS^2 data may be used to determine the acyl group for a given $[M+NH_4]^+$ ion. The exact mass information obtained from the MS^2 spectra can be used in combination with the unfragmented ion to identify possible molecular TG species. Moreover, since in these experiments the two collision cells (Trap T-wave and Transfer T-wave) are used in a parallel fashion to generate the MS^E spectra, it is possible to create a pseudo MS^3 spectrum of all ions. With this in mind, the high energy spectra of the already produced or first generation of product ions (diacyl ions), gave rise to the second generation product ions like the acylium (RCO^+) and the $(RCO+74)^+$ ions. Figure 5A and 5B clearly show the results for the combined spectrum between the low and high energy scans at 8.82 minutes. As it can be observed in the low energy data it is possible to obtain information from precursor ion. The base peak ion is at m/z 874.7885 (+2.4 ppm) which corresponds to TG (52:3). However, at the same retention time there are a number of TG species which co-elute chromatographically. Nevertheless, it is possible to align and recognize the fragment-ions belonging to the unfragmented precursor ion if the co-eluting ions are separated only by a single scan. Having said that, in this particular case we know that we are dealing with TGs due to the elution window in the chromatogram and therefore most of the fragment-ion data will belong to these compounds. It is possible to appreciate that the ions at m/z 601.5197 (loss of 16:0 FA) chain, m/z 577.5194 (loss of 18:2 FA) chain and m/z 575.5036 (loss of the 18:1 FA chain) (Figure 5A) all can be used as diagnostic fragment-ions to identify the presence of the ion at m/z 874.7885 (TG (52:3)). This information is all obtained simultaneously and in the same injection. Figure 5B shows three extracted ion chromatograms at m/z 601.5220, 577.5210 and 575.5040 (window of +/- 30 mDa) a number of chromatographic peaks which are very selective and indicative for these fragment-ions giving indication of the losses of 16:0 FA, 18:2 FA and 18:1 FA chains, respectively. Likewise, the data can be selectively data-mined for specific fragment-ions which correspond to the TG molecular species and confirmed by exact mass in the low energy trace. Exact mass neutral-loss information may also be extracted out of this complex data set for the classification of TGs. There are many different neutral losses which may be used as diagnostic losses for the confirmation of TGs, but in this example we will use one to demonstrate the proof of principle of this powerful analytical strategy. For instance, if the data is interrogated for the loss of the 16:0 FA, corresponding to $[CH_3(CH_2)_{14}CO_2H+NH_3]$ with an exact mass neutral loss of 273.2668, a chromatogram will be obtained showing all precursors displaying this exact mass neutral loss. This is illustrated in more detail in figure 5C, where it is possible to observe how the data can be mined for exact mass neutral losses which correspond to specific FA moieties by comparing the low and high energy acquisitions. The biggest

advantage here is that it is possible to search for an unlimited number of exact mass neutral losses as this methodology is not limited by duty cycle such as in other scanning mass spectrometers.

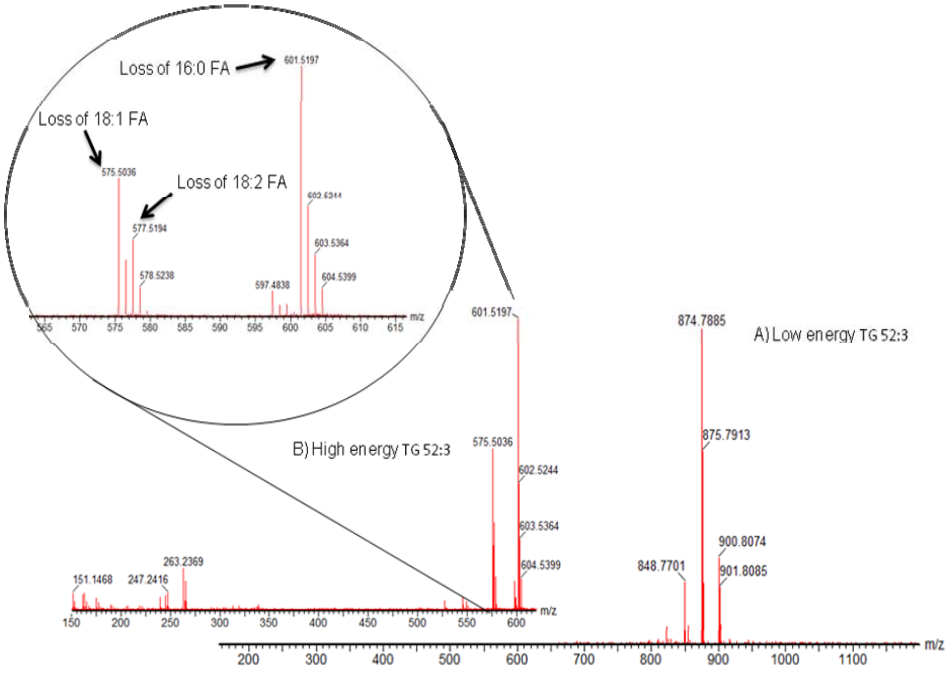

Figure 5A. Shows the low energy (A) for TG (52:3) and the corresponding high energy fragmentation spectra (B) obtained at a retention time of 8.82 min with key diagnostic fragment-ions at m/z 601.5197 (loss of 16:0 FA chain), m/z 577.5194 (loss of 18:2 FA chain) and m/z 575.5036 (loss of the 18:1 FA)

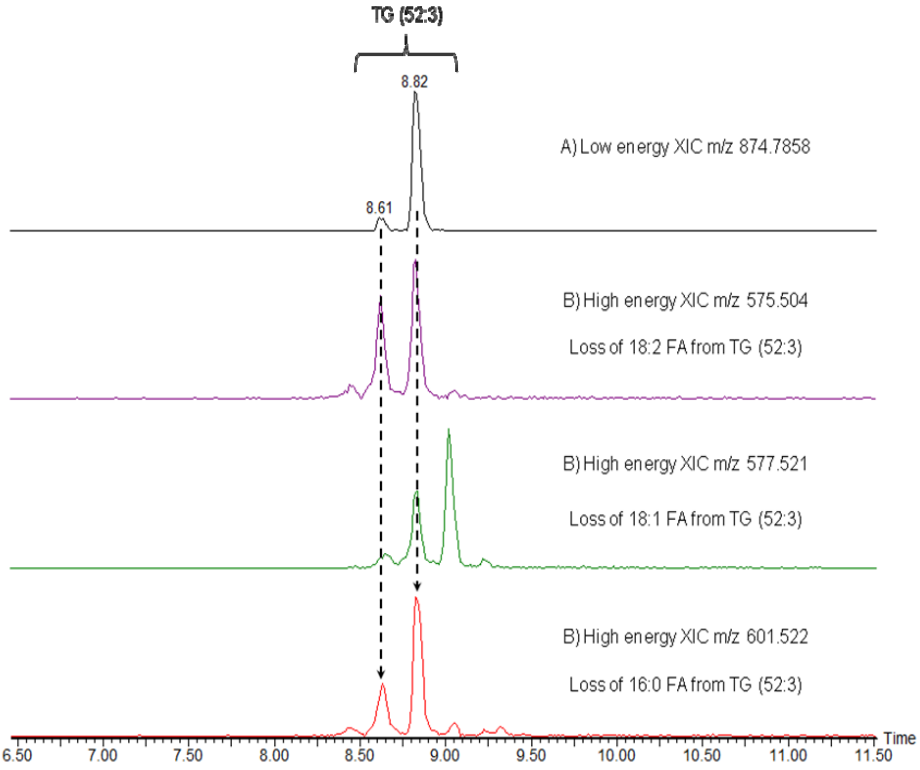

Figure 5B. (A) Low energy extracted ion chromatogram for unfragmented protonated TG (52:3) and (B) high energy extracted ion chromatograms of 'key fragment-ions' which denote losses of acyl FA from the TG (52:3) (m/z 601.5220, loss of 16:0 FA chain; m/z 577.5210, loss of 18:2 FA chain and m/z 575.5040, loss of the 18:1 FA).

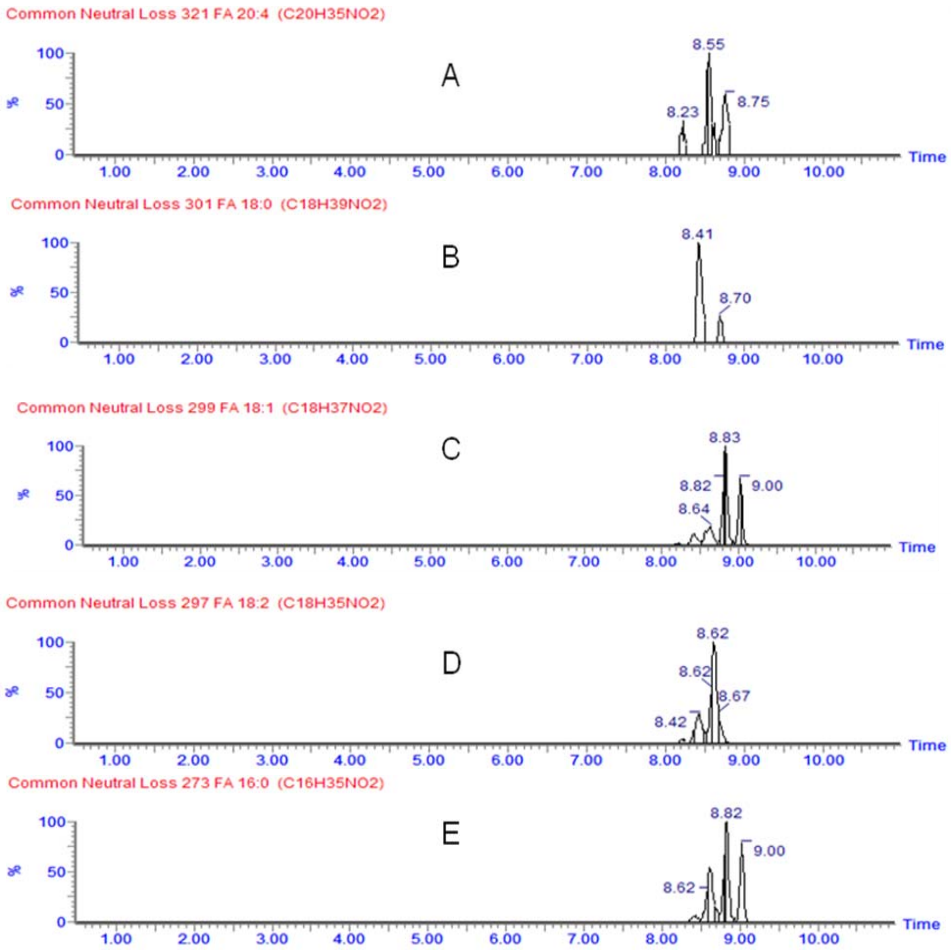

Figure 5C. Use of UPLC-MS^{E} to search for different FA loses using exact mass neutral loss in extracted human plasma sample. The data was processed using MetaboLynx XS. The losses of different FA moieties corresponded to (A) loss of 20:4 FA, (B) loss of 18:0 FA, (C) loss of 18:1 FA, (D) loss of 18:2 FA, (E) loss of 16:0 FA.

With respect to the cholesterol esters (ChoE), these molecular entities are also well detected by electrospray. For these compounds, the ester bond is formed between the carboxylate group of the fatty acid and the hydroxyl group of the cholesterol. These biochemicals are related to atherosclerosis and inborn errors of lipid metabolism. The main characteristics of the (ChoE) under CID is that they give rise to the cholesteryl motif at m/z 369.3516 (Figure 3S supplemental information) which may be used as the key diagnostic fragment-ion to locate and confirm the presence of the different species of ChoE. If the high energy data is interrogated for the diagnostic fragment-ion at m/z 369.3516, then a number of ChoE entities are identified as observed in Figure 6. Major ChoE at m/z 664.6057 (3.6 ppm) at 9.67 minutes,

m/z 666.6193 (0.6 ppm) at 9.84 minutes, m/z 668.6337 (-1.3 ppm) at 10.14 minutes, m/z 668.6016 (-2.4 ppm) at 9.5 minutes, m/z 690 .6189 (0.1 ppm) at 9.72 minutes and m/z 714.6185 (-0.6 ppm) at 9.61 where all identified using the high energy information together using the correlation with the low energy data.

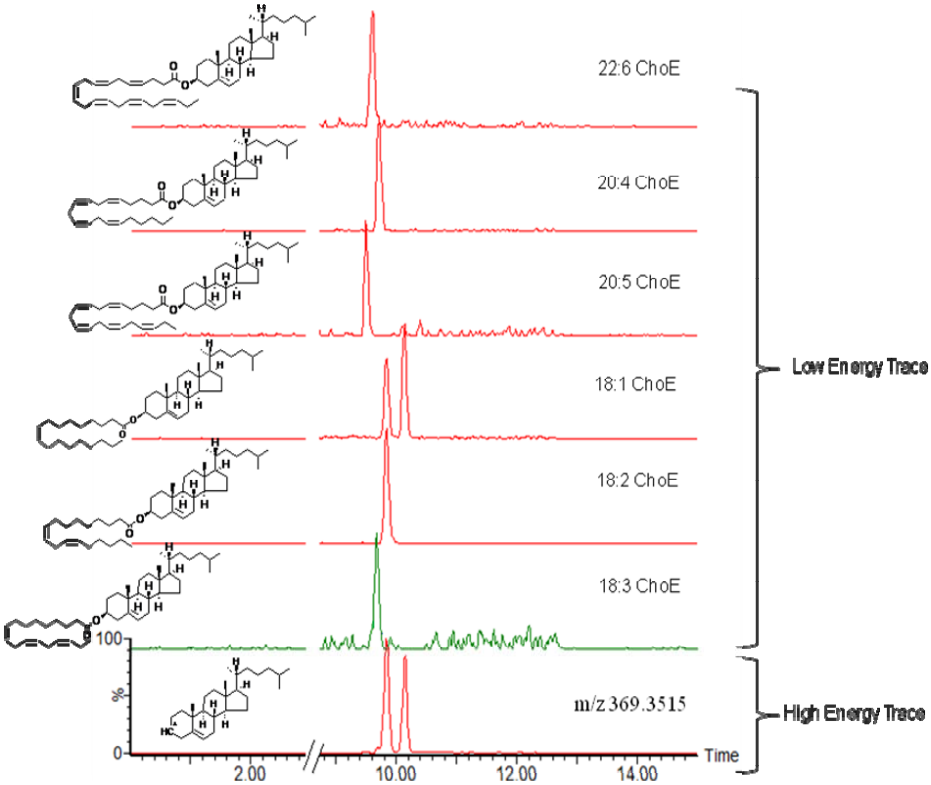

Figure 6. Reconstructed ion chromatograms of UPLC-MS^E data with low and high energy acquisitions. The high energy reconstructed ion chromatogram of the key fragment-ion from the cholesteryl (m/z 369.3515) is used to identify the possible presence of ChoE's, and subsequently at the indicated low energy UPLC-MS trace as the key fragment-ion from the cholesteryl (m/z 369.3515). Following alignment with the low energy trace it is possible to extract the unfragmented ion information, which corresponds to the ChoE. The structures shown are examples of possible structures.

In electrospray negative ion mode, complementary information is obtained. More specifically, under CID anions or deprotonated molecules of glycerophospholipids produce important and abundant acyl anions of their FA moieties. In this mode of operation and applying MS^E it is possible to simultaneously profile in a parallel fashion for the FA elemental composition in a large number of molecular species which may be present in any lipid extract. In Figure S4 (supplemental information) this is demonstrated for the extracted high energy precursor ion chromatograms of several fatty acids, i.e. FA 15:0 (precursor ion *m/z* 241.2175), FA 16:0 (precursor ion *m/z* 255.2332,), FA 18:2 (precursor ion *m/z* 279.2332), FA 18:1

(precursor ion *m/z* 281.2489), FA 18:0 (precursor ion *m/z* 283.2646) and FA 20:4 (precursor ion *m/z* 303.2332). For this different FA's the corresponding unfragmented precursor ion could be found in the low-energy trace. An example shown in Figure S5 (supplemental information) where the peak at a retention time of 4.25 minutes for both the low and the high energy corresponded to the calibration standard PG 14:0/14:0. This acidic glycerophospholipid is preferentially ionized in negative electrospray ion mode. In this mode, it yields the $[M-H]^-$ ion as most abundant ion. The fragment-ions obtained by CID yield similar fragments as described for other glycerophospholipid classes such as product ions arising from the following fragmentation mechanisms; a) neutral losses of the free FA ($[M-H-R_nCOOH]^-$), b) neutral losses of ketenes ($[M-H-R'_nCH=C=O]^-$), or from the carboxylate anion fragments $(R_nCOO)^-$. Additionally, PG fragment-ions also give rise to a specific fragment-ion at m/z 227 which corresponds to the $(glycerophosphoglycerol-H-H_2O)^-$. This fragment-ion can be used as a descriptor in electrospray negative ion mode to search for PG's. Figure 7 highlights how this information is obtained in the high energy collision mode where the key fragment-ions at m/z 227.2003 (-3.5 ppm) corresponding to either the $[sn1-H]^-$ acid or $[sn2-H]^-$ acid, m/z 437.2298 (-1.4 ppm) corresponding to either the $[(M-sn-1-H_2O)-H]^-$ or $[(M-sn-2-H_2O)-H]^-$, m/z 455.2420 (2.2 ppm) corresponding to either the $[(M-sn-1)-H]^-$ or $[(M-sn-2)-H]^-$are generated. The presence of these key diagnostic fragment-ions for the PG together with the exact mass in the low and high energy traces at the same retention time was enough for a positive identification of this type of glycerophospholipid confirming it to the PG 14:0/14:0 at m/z 665.4406 (1.8 ppm).

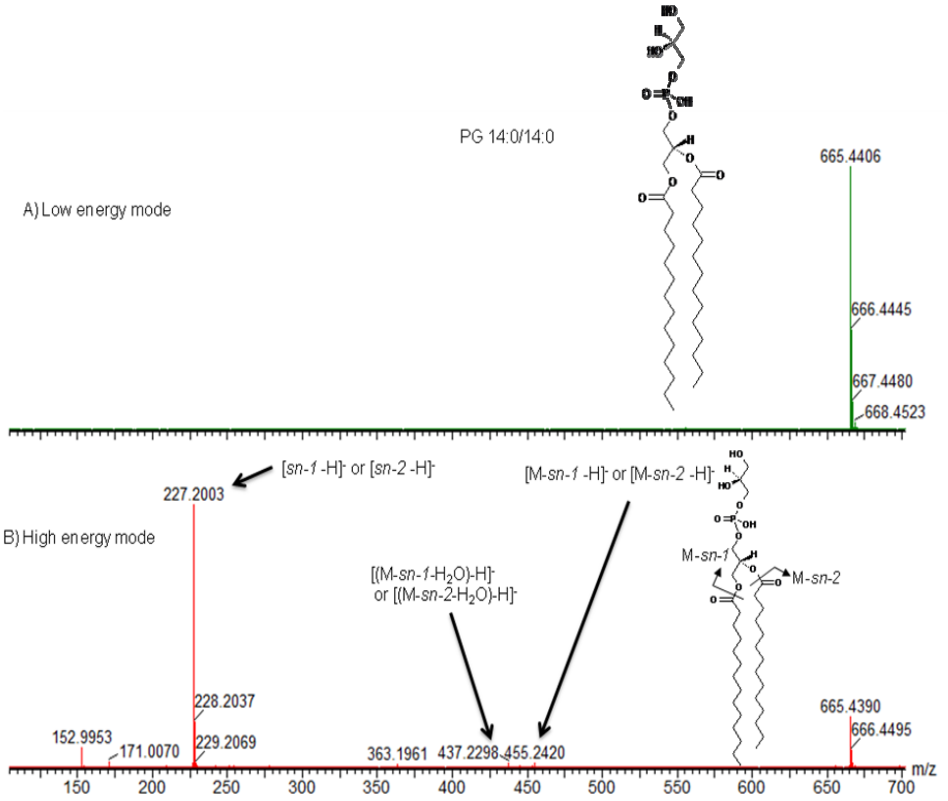

Figure 7. Low energy spectra (A) and the fragment-ions in the high energy mode (B) of PG 14:0/14:0 (negative ionization mode)

"Shotgun Lipidomic" Method Application: Osteoarthritis Samples

The potential of the lipidomic method was explored for the discovery of biomarkers for OA. Plasma samples from patients with various levels of OA were analyzed to detect and identify putative lipids which may be able to differentiate between the different levels of OA. Usually the first chemometrical tool used in the evaluation of a metabolomics study is Principal Component Analysis (PCA) to provide a fast overview of the most important variations and differences between objects. PCA as an unsupervised data analysis (40) technique did not provide an obvious separation between the groups with different stages of OA (data not shown). For the statistical data analysis, the individual data sets for each subject was organized in 3 groups; Control was comprised of group 0, Early OA contained groups 1-2, Moderate OA contained groups 3-8. The created model was evaluated by inspecting the goodness of fit (R^2X) and predictive power (Q^2X) with values of 0.41 and 0.30 respectively. In order to localize subtle differences between the groups, partial least squares-discrimination analysis (PLS-DA) was used for data analysis. After applying this methodology, it was possible to obtain a

significant separation between all the different groups that is; the control sample, the early OA and the moderate OA (Figure 8).

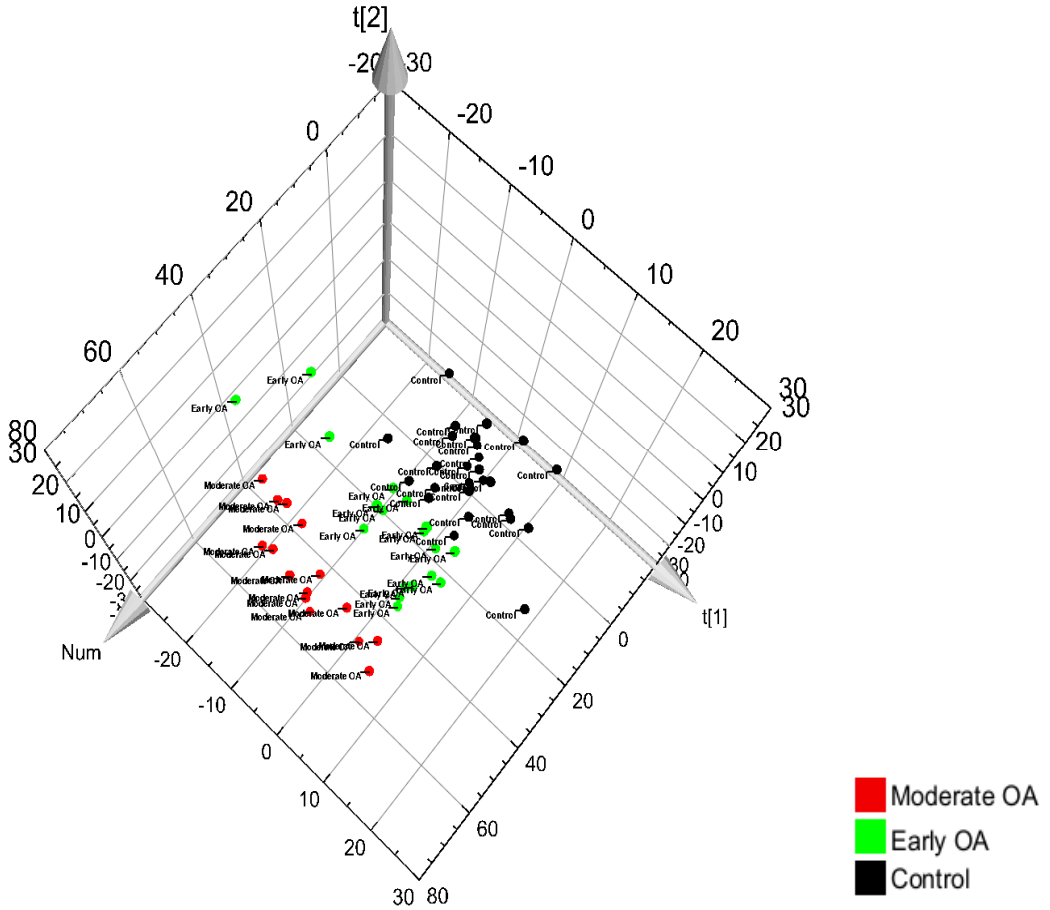

Figure 8. Partial Least Squares- Discrimination Analysis (PLS-DA) score plot of different OA samples of different disease state (Control, Early OA, and Moderate OA).

These results suggest that altered lipid metabolism is involved in OA. In OA, inflammatory pain is a typical occurrence. Phospholipases A_1 and A_2 hydrolyze the *sn-1*(PLA_1) or *sn-2* (PLA_2) acyl bond of phospholipids, for example arachidonic acid (41) (C20:4) is released from a PC that contains a C20:4 acyl FA chain. As a consequence of this reaction, arachidonic acid is formed together with a corresponding lysophospholipid. Arachidonic acid is an inflammatory mediator, and therefore an increased activity of Phospholipase can be expected in the case of inflammation. The activity of the Phospholipase enzyme was gauged by monitoring the ratios between LPC (16:0) /PC (36:4) and LPC (18:0) /PC

(38:4). In the extracted ion chromatograms (low energy trace) of the protonated PC 36:4 and the PC 38:4 a number of isomers showed up as chromatographically separated peaks. In order to include only those PC's which did contain FA 20:4, the high energy data were used to determine those isomers which contained FA 20:4 in either the *sn-1* or *sn-2* position. By monitoring the ratio of the sum of the normalized response of LPC 16:0 and LPC 18:0 and the sum of the response of PC 36:4 and PC 38:4 it can be observed that there was a considerable change of the ratio; this change indicated an changed activity of Phospholipase from control to early OA and moderate OA. This latter showed an increased level in the ratio of LPC/PC as noted with respect to the controls but not as elevated as in early OA (Figure 9).

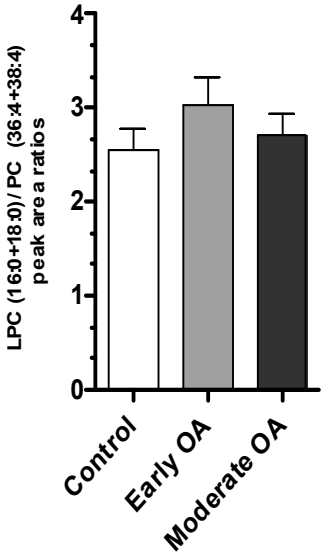

Figure 9. Shows the absolute peak area ratio between LPC (16:0+18:0) / PC (36:4+38:4) for the entire study in all groups (Control, Early OA and Moderate OA). The error bar spread indicates the biological standard deviation of all results for the subjects in each group.

CONCLUSIONS

The usefulness of MS^E as an untargeted methodology for both quantitation and identification in the same analysis has been clearly demonstrated. We applied this approach to lipid profiling but any other biochemicals which may be present in the biological sample could have been monitored in a comparable manner. The qualitative data allowed for the unambiguous identification of FA chain lengths. In principle *all* individual phospholipids and di- and triglycerides, whereas similar LC-MS/MS techniques such as data dependent acquisitions have limitations with respect to coverage for complex samples as the ones studied here. Data dependent analysis would simply miss various lipids due to time constraints and complexity of the samples; different lipids fragment according to different fragmentation mechanisms generating a vast number of different key fragment-ions and specific neutral losses in either positive or negative ion electrospray based techniques. MS^E on the other hand acquires all relevant information in both low energy and high energy acquisitions during the same analysis, and in the subsequent data processing available information on fragmentation pathways, diagnostic precursor and neutral losses allowed us to determine the polar head group and FA composition in a relatively fast and efficient manner.

This analytical strategy has been successfully applied to a study changes in the lipid profile in patients with a different degree of osteoarthritis. In summary, the capabilities of the combination of efficient separation using UPLC combined with detection using a TOF-MS in MS^E mode has been clearly demonstrated for the analysis of a wide range of lipids.

REFERENCES

1. Dowhan, W.; Bogdanov, M. pp. 1-35 (edited by D.E. Vance and J.E. Vance, Elsevier Science) **2002**.
2. Wenk, M. R. *Nat. Rev. Drug Discovery* **2005**, *4*, 594–610.
3. Feng, L.; Prestwich, G.D. (Dekker-CRC, New York, **2005**).
4. Eyster,K.M. *Adv. Physiol. Edu*., **2007,** *31*, 5-16.
5. Jakobsson, A.; Westerberg, R. *Prog. Lipid Res*., **2006**, *45*, 237-249
6. Endo, A. *J. Lipid Res.* **1992**, *33* (11): 1569–82.
7. Fahy, E.; Subramaniam, S.; Brown, H.A.; Glass, C.K.; Merrill, A.H.; Murphy, R.C.; Raetz, C.R.H.; Russell, D.W.; Seyama, Y.; Shaw, W.; Shimizu, T.; Spener F.; Van Meer, G.; Vannieuwenhze, M.S.; White, S.H.; Witztum, J.L.; Dennis, E.A. *Journal of Lipid Research*. **2005**, *46*, 839-861.
8. Goni, F. M.; Alonso, A. (eds Muller, G. & Petry, S.) 79–100 (Wiley-VCH, Weinheim, Germany, **2004**).
9. Athenstaedt, K.; Daum, G. *Eur. J. Biochem.* **1999**, *266*, 1–16
10. Balazy, M. *Prostaglandins Other Lipid Mediat.* **(2004)** , *73*, 173–180
11. Pettus, B. J.; Chalfant, C. E.; Hannun, Y. A. *Curr. Mol. Med.* **2004**, *4*, 405–418.
12. Reynolds, C. P.; Maurer, B. J; Kolesnick, R. N. *Cancer Lett.* **2004**, *206*, 169–180
13. Hla, T. *Semin. Cell Dev. Biol.* **2004**, *15*, 513–520.
14. Muller, G. Lipases and Phospholipases in Drug Development 231–331 (Wiley-VCH, Weinheim, Germany, **2004**).
15. Hollander, P. *Prim. Care* **2003**, *30*, 427–440.
16. Laaksonen, R.; Katajamaa, M.; Paiva, H.; Sysi.Aho, M.; Saarinen, L.; Junni, P.; Lutjohann, D.; Smet, J.; Van Coster, R.; Seppanen-Laakso, T.; Lehtimaki, T.; Soini, J.; Oresic, M. *PLoS One* **2006**, *1* (1), e97.
17. Nagan, N.; R.A. Zoeller. *Progress in Lipid Research*. **2001**, *40*, 199-229.
18. Tiller PR.; Yu S., Castro-Perez J.; Fillgrove KL.; Baillie TA .*Rapid Commun. Mass Spectrom.* **2008**, *22,* 1053-1061.

19. Yu, K.; Di L.; Kern,s E.; Li, S.Q.; Alden, P.; Plumb, S.R.. *Rapid Communications in MassSpectrometry* **2007**, *21*, Issue 6, 893-902.

20. Plumb, R.S.; Johnson, K.A.; Rainville, P.; Shockcor, J.P.; Williams, R.; Granger, J.H.; Wilson, I.D. *Rapid Communications in MassSpectrometry*. **2006** , *20*, Issue 19, 2800-2806.

21. Fenn, J.B.; Mann, M.; Meng, C.K.; Wong, S.F.; Whitehouse, C.M. *Science*, **1989**, *246*:64-71.

22. Watkins, S. M. *Curr. Opin. Drug Discov. Devel.* **2004**, *7*, 112–117.

23. Houjou, T.; Yamatani, K.; Imagawa, M.; Shimizu, T.; Taguchi, R. *Rapid Commun. Mass Spectrom.* **2005**, *19*, 654–666.

24. Hermansson, M.; Uphoff, A.; Kakela, R.; Somerharju, P. *Anal. Chem.* **2005**, *77*, 2166–2175.

25. Han, X.; Gross, R. W. *Anal. Biochem.* **2001**, *295*, 88–100.

26. Sullards, M. C.; Merrill, A. H. Jr. *Sci STKE* PL1 , **2001**.

27. Wenk, M. R.; Lucast, L.; Di Paolo, G.; Romanelli, AJ.; Suchy, SF.; Nussbaum, RL.; Cline, GW.; Shulman, GI.; McMurray, W; De Camilli, P. *Nature Biotechnol.* **2003**, *21*, 813–817.

28. Ekroos, K.; Chernushevich, I. V.; Simons, K.; Shevchenko, A. *Anal. Chem.* **2002**, *74*, 941–949.

29. Wrona, M.; Mauriala, T.; Bateman, K.P.; Mortishire-Smith, R.J.; O'Connor, D. *Rapid Communications in Mass Spectrometry* . **2005**, 19, Issue 18, 2597-2602.

30. Bateman, K.P.; Castro-Perez, J.; Wrona, M.; Shockcor, J.P.; Yu, K.; Oballa R., Nicoll-Griffith, D.A . *Rapid Communications in Mass Spectrometry* **2007**, *21*, Issue 9, 1485-1496.

31. Rainville, P. D.; Stumpf, C. J.; Shockcor, J. P.; Plumb, R. S.; Nicholson, J. K. *J. Proteome Res.* **2007**, *6*, 552–558.

32. Bligh, E.G.;Dyer, W.J. *Can. J. Biochem. Psysiol* **1959**, *37*,911-917

33. Wesseling, J.; Dekker, J.; van den Berg, WB.; Bierma-Zeinstra, SM.; Boers M, Cats HA.; Deckers, P.; Gorter, KJ.; Heuts, PH.; Hilberdink, WK.; Kloppenburg, M.; Nelissen, RG.; Oosterveld, FG.; Oostveen, JC.; Roorda, LD.; Viergever, MA.; Ten Wolde, S.; Lafeber, FP.; Bijlsma, JW. *Ann Rheum Dis*. **2009** , *68* (9), 1413-9

34. Hsu, F.F.; Bohrer, A.; Turk, J. *J. Am. Soc. Mass Spectrom.* **1998** ,*9* , 516-526

35. Hsu, F.F.; Turk, J. *J. Am. Soc. Mass Spectrom.* **2003**, *14,* 352-363.

36. Barroso, B.; Bischoff, R. *J. Chromatogr., B* **2005**, *814*, 21–28.

37. Laaksonen, R.; Katajamaa, M.; Paiva, H.; Sysi.Aho, M.; Saarinen, L.; Junni, P.; Lutjohann, D.; Smet, J.; Van Coster, R.; Seppanen-Laakso, T.; Lehtimaki, T.; Soini, J.; Oresic, M. *PLoS One* **2006**, *1* (1), e97.

38. Chunxiu, H,.; van Dommelen, J.; van der Heijden, R.; Spijksma, G.; Reijmers, T. H.; Wang, M.; Slee, E.; Lu, X.; Xu, G.; van der Greef, J.; Hankemeier, T. *Journal of Proteome Research*. **2009**, *7*, 4982–4991.

39. Ding, J.; Sorensen, C.M.; Jaitly, N.; Jiang, H.; Orton, D.J.; Monroe, M.E.; Moore, R.J.; Smith, R.D.; Metz, T.O. *Journal of Chromatography B*, **2008**, *871* ,243-252.

40. Hsu, F.F.; Turk, J.; Thukkanni,A.K.; Messner, M.C.; Wildsmith, K.R.; Ford, D.A. *J. Am. Soc. Mass Spectrom.* **2003**, *38*, 752-763.

41. Murphy, R.C.; Wu, C.C.; MacAnoy, A.M. *J Am Soc Mass Spectrom* **2005**, *16*, 1498-1509

42. Jackson, J. E. *A User's Guide to Principal Components*; Wiley: New York, **1991**.

43. Macrides, TA; Treschow, AP. Abstract, 88th American Oil Chemists Society.

SUPPLEMENTARY INFORMATION

Supplemental Figure S1. Intraday and interday variation bar chart for all non-endogenous lipids used in the validation set

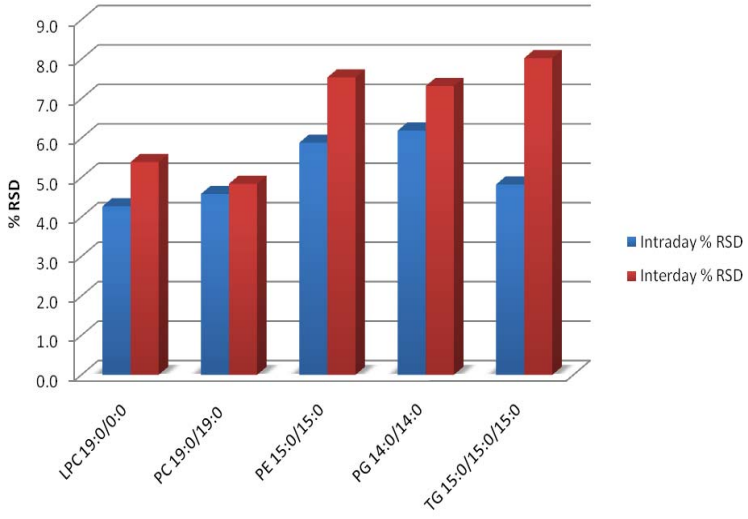

Supplemental Figure S2. Recovery for all non-endogenous lipids used in the validation set during three consecutive days

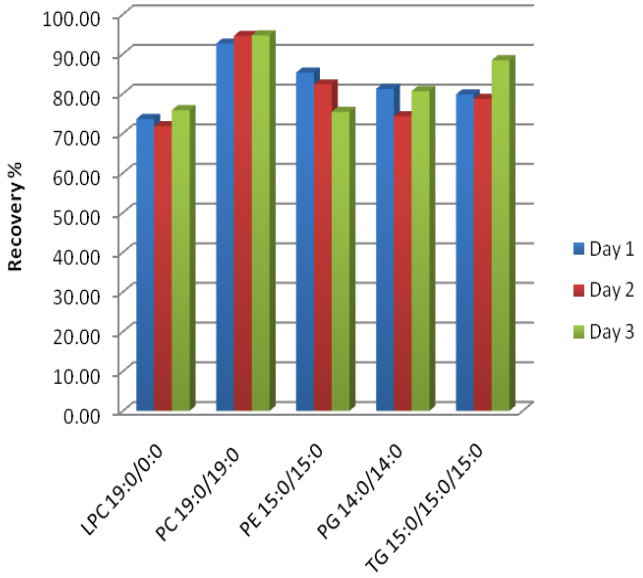

Table S1. List of all major lipids identified in the human extracted plasma; the m/z of the most abundant ion, the mass error, retention time, provisional lipid assignment and the ionization mode (positive/negative) are given.

Class	Formula	m/z Found	ppm	Time (min)	provisional assignment class		Ionization mode
ChoE	C47H77NO2	688.6016	-2.4	9.5	ChoE	20:5	$[M+NH_4]^+$
	C49H79NO2	714.6185	-0.6	9.61	ChoE	22:6	$[M+NH_4]^+$
	C45H77NO2	664.6057	3.6	9.67	ChoE	18:3	$[M+NH_4]^+$
	C47H79NO2	690.6189	0.1	9.72	ChoE	20:4	$[M+NH_4]^+$
	C45H79NO2	666.6193	0.6	9.84	ChoE	18:2	$[M+NH_4]^+$
	C45H81NO2	668.6337	-1.3	10.14	ChoE	18:1	$[M+NH_4]^+$
DG	C39H71NO5	634.5411	0	6.41	DG	36:4	$[M+NH_4]^+$
FA	C18H30O2	277.2150	-6.4	1.46	FA	18:3	[M-H]-
	C22H32O2	327.2301	-7.1	1.52	FA	22:6	[M-H]-
	C14H28O2	227.2023	5.1	1.55	FA	14:0	[M-H]-
	C16H30O2	253.2170	0.9	1.65	FA	16:1	[M-H]-
	C20H32O2	303.2309	-5	1.7	FA	20:4	[M-H]-
	C18H32O2	279.2319	-1.9	1.8	FA	18:2	[M-H]-
	C20H34O2	305.2476	-1.6	1.98	FA	20:3	[M-H]-
	C16H32O2	255.2324	-0.1	2.12	FA	16:0	[M-H]-
	C22H36O2	331.2635	-0.7	2.18	FA	22:4	[M-H]-
	C18H34O2	281.2479	-0.6	2.24	FA	18:1	[M-H]-
	C17H34O2	269.2484	1.2	2.47	FA	17:0	[M-H]-
	C18H36O2	283.2638	0.2	2.86	FA	18:0	[M-H]-
	C20H38O2	309.2786	-2.5	2.95	FA	20:1	[M-H]-
	C20H40O2	311.2971	6.6	3.68	FA	20:0	[M-H]-
PC	C42H76NO8P	754.5411	3.2	4.89	PC	34:4	$[M+H]^+$
	C40H76NO8P	730.5409	3.1	4.4	PC	32:2	$[M+H]^+$
	C44H78NO8P	780.5551	1	4.54	PC	36:5	$[M+H]^+$
	C46H76NO8P	802.5403	2	4.54	PC	38:8	$[M+H]^+$
	C46H80NO8P	806.5709	1.2	4.55	PC	38:6	$[M+H]^+$
	C44H76NO8P	778.5371	-2.1	4.59	PC	36:6	$[M+H]^+$
	C44H80NO8P	782.5715	2	4.62	PC	36:4	$[M+H]^+$
	C42H78NO8P	756.5535	-1.1	4.71	PC	34:3	$[M+H]^+$

C42H82NO7P	744.5935	3.8	4.71	PC-plasm	34:1	$[M+H]^+$
C44H80NO8P	782.5718	2.4	4.78	PC	36:4	$[M+H]^+$
C46H80NO8P	806.5729	3.7	4.78	PC	38:6	$[M+H]^+$
C40H78NO8P	732.5576	4.5	4.89	PC	32:1	$[M+H]^+$
C46H78NO8P	804.5527	-2	4.93	PC	37:0	$[M+H]^+$
C44H80NO8P	782.5728	3.6	4.94	PC	36:4	$[M+H]^+$
C35H70NO8P	664.4935	2.7	4.96	PC	28:7	$[M+H]^+$
C46H82NO8P	808.5896	4.9	4.96	PC	38:5	$[M+H]^+$
C42H80NO8P	758.5718	2.4	5.02	PC	34:2	$[M+H]^+$
C44H78NO8P	780.5545	0.2	5.04	PC	36:5	$[M+H]^+$
C44H82NO8P	784.5876	2.5	5.09	PC	36:3	$[M+H]^+$
C44H80NO7P	766.5762	1.4	5.15	PC-plasm	36:4	$[M+H]^+$
C44H82NO8P	784.5876	2.5	5.15	PC	36:3	$[M+H]^+$
C46H82NO8P	808.5851	-0.6	5.15	PC	38:5	$[M+H]^+$
C46H80NO8P	806.5684	-1.9	5.18	PC	38:6	$[M+H]^+$
C43H82NO8P	772.5861	0.6	5.22	PC	35:2	$[M+H]^+$
C46H82NO7P	792.5931	3	5.23	PC-plasm	38:5	$[M+H]^+$
C45H82NO8P	796.5875	2.4	5.23	PC	37:4	$[M+H]^+$
C46H84NO8P	810.6044	3.9	5.23	PC	38:4	$[M+H]^+$
C48H82NO8P	832.5808	-5.8	5.23	PC	39:0	$[M+H]^+$
C46H80NO7P	790.5731	-2.5	5.3	PC-plasm	38:6	$[M+H]^+$
C43H82NO8P	772.5858	0.2	5.31	PC	35:2	$[M+H]^+$
C44H78NO7P	764.5595	0.1	5.32	PC-plasm	36:5	$[M+H]^+$
C46H84NO8P	810.6016	0.4	5.35	PC	38:4	$[M+H]^+$
C48H84NO8P	834.6031	2.2	5.36	PC	40:6	$[M+H]^+$
C40H80NO8P	734.5718	2.5	5.43	PC	32:0	$[M+H]^+$
C44H84NO7P	770.6059	-0.6	5.43	PC-plasm	36:2	$[M+H]^+$
C46H84NO7P	794.6064	0	5.43	PC-plasm	38:4	$[M+H]^+$
C42H82NO8P	760.5883	3.5	5.44	PC	34:1	$[M+H]^+$
C48H86NO7P	820.6230	1.2	5.44	PC-plasm	40:5	$[M+H]^+$
C44H80NO8P	782.5695	-0.6	5.45	PC	36:4	$[M+H]^+$
C46H84NO8P	810.6037	3	5.51	PC	38:4	$[M+H]^+$
C48H82NO8P	832.5830	-3.1	5.51	PC	40:7	$[M+H]^+$
C48H86NO8P	836.6119	-6	5.51	PC	40:5	$[M+H]^+$

	C46H82NO8P	808.5830	-3.2	5.58	PC	38:5	$[M+H]^+$
	C44H84NO8P	786.6025	1.6	5.59	PC	36:2	$[M+H]^+$
	C43H78NO8P	768.5568	3.2	5.66	PC	35:4	$[M+H]^+$
	C43H84NO8P	774.6008	-0.6	5.71	PC	35:1	$[M+H]^+$
	C42H84NO7P	746.6033	-4.2	5.72	PC-plasm	34:0	$[M+H]^+$
	C46H86NO8P	812.6152	-2.1	5.72	PC	38:3	$[M+H]^+$
	C48H84NO8P	834.5981	-3.8	5.72	PC	40:6	$[M+H]^+$
	C42H84NO8P	762.6032	2.6	5.91	PC	34:0	$[M+H]^+$
	C44H82NO8P	784.5865	1.1	5.91	PC	36:3	$[M+H]^+$
	C44H86NO8P	788.6165	-0.5	5.98	PC	36:1	$[M+H]^+$
	C46H84NO8P	810.5992	-2.5	5.98	PC	38:4	$[M+H]^+$
	C46H88NO8P	814.6338	1.5	6.03	PC	38:2	$[M+H]^+$
	C41H76NO8P	742.5365	-2.9	6.06	PC	33:3	$[M+H]^+$
	C39H78NO8P	720.5533	-1.4	6.06	PC	31:0	$[M+H]^+$
	C46H92NO8P	818.6649	1.3	6.83	PC	38:0	$[M+H]^+$
	C52H96NO8P	894.6934	-2	8.44	PC	44:4	$[M+H]^+$
	C50H96NO8P	870.6982	3.5	8.57	PC	42:2	$[M+H]^+$
	C52H98NO8P	896.7118	1.1	8.6	PC	44:3	$[M+H]^+$
	C52H100NO8P	898.7225	-4.4	8.82	PC	44:2	$[M+H]^+$
	C54H102NO8P	924.7462	4.4	8.83	PC	46:3	$[M+H]^+$
	C48H94NO8P	844.6763	-3.8	8.9	PC	40:2	$[M+H]^+$
	C52H102NO8P	900.7373	-5.3	9.02	PC	44:1	$[M+H]^+$
	C54H106NO8P	928.7690	-4.8	9.21	PC	46:1	$[M+H]^+$
PE	C43H76NO8P	764.5237	0.8	5.16	PE	38:5	[M-H]-
	C39H74NO8P	714.5103	4	5.18	PE	34:2	[M-H]-
	C43H78NO8P	766.5403	2.1	5.65	PE	38:4	[M-H]-
	C41H78NO8P	742.5404	2.3	5.74	PE	36:2	[M-H]-
PG	C32H63O10P	637.4073	-1.2	2.79	PG	26:0	[M-H]-
	C36H71O10P	693.4739	4.6	4	PG	30:0	[M-H]-
	C52H99O10P	913.6851	-5.1	6.26	PG	46:2	[M-H]-
PI	C45H79O13P	857.5202	2.5	3.99	PI	36:4	[M-H]-
	C43H79O13P	833.5187	0.8	4.07	PI	34:2	[M-H]-
	C49H83O13P	909.5511	1.9	4.42	PI	40:6	[M-H]-
	C43H81O13P	835.5377	4.8	4.5	PI	34:1	[M-H]-

	C47H83O13P	885.5524	3.5	4.57	PI	38:4	[M-H]-
	C45H83O13P	861.5481	-1.4	4.64	PI	36:2	[M-H]-
	C47H85O13P	887.5643	-0.8	4.76	PI	38:3	[M-H]-
PS	C37H72NO10P	720.4839	3.2	4.11	PS	31:0	[M-H]-
	C44H80NO10P	812.5402	-4.9	4.32	PS	38:3	[M-H]-
	C42H80NO10P	788.5465	2.9	4.42	PS	36:1	[M-H]-
	C46H82NO10P	838.5621	2.7	4.42	PS	40:4	[M-H]-
	C44H82NO10P	814.5624	3.1	4.53	PS	38:2	[M-H]-
	C46H82NO10P	838.5647	5.8	4.56	PS	40:4	[M-H]-
	C48H84NO10P	864.5773	2.1	4.56	PS	42:5	[M-H]-
	C46H84NO10P	840.5766	1.3	4.66	PS	40:3	[M-H]-
	C43H82NO10P	802.5607	1.1	4.73	PS	37:1	[M-H]-
	C48H84NO10P	864.5776	2.4	4.79	PS	42:5	[M-H]-
	C39H72NO10P	744.4801	-2	4.96	PS	33:2	[M-H]-
	C48H86NO10P	866.5933	2.5	4.98	PS	42:4	[M-H]-
	C44H84NO10P	816.5768	1.6	5.05	PS	38:1	[M-H]-
	C46H86NO10P	842.5944	3.9	5.11	PS	40:2	[M-H]-
	C48H86NO10P	866.5925	1.6	5.16	PS	42:4	[M-H]-
	C46H86NO10P	842.5911	0	5.19	PS	40:2	[M-H]-
	C45H86NO10P	830.5872	-4.7	5.26	PS	39:1	[M-H]-
	C45H86NO10P	830.5933	2.6	5.31	PS	39:1	[M-H]-
	C46H86NO10P	842.5946	4.1	5.37	PS	40:2	[M-H]-
	C50H88NO10P	892.6071	0.4	5.37	PS	44:5	[M-H]-
	C44H86NO10P	818.5949	4.6	5.46	PS	38:0	[M-H]-
	C48H88NO10P	868.6103	4	5.53	PS	42:3	[M-H]-
	C50H90NO10P	894.6236	1.3	5.54	PS	44:4	[M-H]-
	C45H86NO10P	830.5903	-1	5.61	PS	39:1	[M-H]-
	C46H88NO10P	844.6032	-4.2	5.61	PS	40:1	[M-H]-
	C50H90NO10P	894.6234	1.1	5.72	PS	44:4	[M-H]-
	C48H90NO10P	870.6227	0.3	5.74	PS	42:2	[M-H]-
	C45H88NO10P	832.6057	-1.3	5.77	PS	39:0	[M-H]-
	C50H92NO10P	896.6399	2	5.91	PS	44:3	[M-H]-
	C46H90NO10P	846.6190	-4.1	6.01	PS	40:0	[M-H]-
	C43H80NO10P	800.5396	-5.7	6.08	PS	37:2	[M-H]-

LPC	C24H48NO7P	494.3251	0.8	1.15	LPC	16:1	$[M+H]^+$
	C28H48NO7P	542.3225	-4.1	1.21	LPC	20:5	$[M+H]^+$
	C22H47NO7P	468.3079	-2.3	1.21	LPC	14:0	$[M+H]^+$
	C26H50NO7P	520.3397	-1.1	1.21	LPC	18:2	$[M+H]^+$
	C30H50NO7P	568.3428	4.4	1.22	LPC	22:6	$[M+H]^+$
	C28H50NO7P	544.3421	3.3	1.23	LPC	20:4	$[M+H]^+$
	C26H50NO7P	520.3394	-1.7	1.26	LPC	18:2	$[M+H]^+$
	C23H48NO7P	482.3244	-0.6	1.42	LPC	15:0	$[M+H]^+$
	C26H48NO7P	518.3246	-0.1	1.43	LPC	18:3	$[M+H]^+$
	C24H50NO7P	496.3399	-0.8	1.45	LPC	16:0	$[M+H]^+$
	C26H52NO7P	522.3538	-4.1	1.57	LPC	18:1	$[M+H]^+$
	C25H52NO7P	510.3568	1.7	1.69	LPC	17:0	$[M+H]^+$
	C27H50NO7P	532.3395	-1.5	1.69	LPC	19:3	$[M+H]^+$
	C26H54NO7P	524.3726	1.9	1.84	LPC	18:0	$[M+H]^+$
	C24H50NO6P	480.3436	-3.7	1.88	LPC	15:1	$[M+H]^+$
	C24H52NO6P	482.3603	-1.7	1.93	LPC	15:0	$[M+H]^+$
	C26H54NO7P	524.3726	1.9	1.97	LPC	18:0	$[M+H]^+$
	C28H52NO7P	546.3549	-1.9	1.99	LPC	20:3	$[M+H]^+$
	C28H52NO7P	546.3559	-0.1	2.02	LPC	20:3	$[M+H]^+$
	C26H54NO6P	508.3758	-1.8	2.06	LPC	17:1	$[M+H]^+$
	C27H56NO7P	538.3885	2.3	2.14	LPC	19:0	$[M+H]^+$
	C27H56NO7P	538.3873	0.1	2.27	LPC	19:0	$[M+H]^+$
LPE	C27H44NO7P	524.2787	1.9	1.21	LPE	22:6	[M-H]-
	C25H44NO7P	500.2798	4.2	1.25	LPE	20:4	[M-H]-
SM	C37H75N2O6P	675.5440	-0.1	4.7	SM	14:0	$[M+H]^+$
	C39H77N2O6P	701.5564	-4.7	4.23	SM	16:1	$[M+H]^+$
	C41H75N2O6P	723.5447	0.9	4.23	SM	18:4	$[M+H]^+$
	C38H77N2O6P	689.5617	2.9	4.45	SM	15:0	$[M+H]^+$
	C39H79N2O6P	703.5767	1.9	4.78	SM	16:0	$[M+H]^+$
	C41H77N2O6P	725.5600	0.4	4.78	SM	18:3	$[M+H]^+$
	C41H81N2O6P	729.5917	0.9	4.89	SM	18:1	$[M+H]^+$
	C43H79N2O6P	751.5771	2.3	4.89	SM	20:4	$[M+H]^+$
	C43H81N2O6P	753.5944	4.5	5.39	SM	20:3	$[M+H]^+$
	C40H81N2O6P	717.5898	-1.8	5.71	SM	17:0	$[M+H]^+$

	C47H87N2O6P	807.6346	-4.2	5.96	SM	24:4	$[M+H]^+$
	C43H87N2O6P	759.6407	3.6	5.98	SM	20:0	$[M+H]^+$
	C41H83N2O6P	731.6089	3	6	SM	18:0	$[M+H]^+$
	C47H91N2O6P	811.6653	-4.9	6.02	SM	24:2	$[M+H]^+$
	C49H89N2O6P	833.6518	-2.2	6.02	SM	26:5	$[M+H]^+$
	C47H87N2O6P	807.6377	-0.3	6.03	SM	24:4	$[M+H]^+$
	C45H89N2O6P	785.6536	0	6.06	SM	22:1	$[M+H]^+$
	C43H85N2O6P	757.6225	0.1	6.12	SM	20:1	$[M+H]^+$
	C37H63N2O6P	663.4521	2.9	6.18	SM	14:6	$[M+H]^+$
	C46H91N2O6P	799.6657	-4.5	6.2	SM	23:1	$[M+H]^+$
	C44H89N2O6P	773.6563	3.5	6.24	SM	21:0	$[M+H]^+$
	C46H91N2O6P	799.6701	1	6.3	SM	23:1	$[M+H]^+$
	C47H93N2O6P	813.6838	-1.4	6.43	SM	24:1	$[M+H]^+$
	C49H91N2O6P	835.6685	-0.9	6.43	SM	26:4	$[M+H]^+$
	C45H91N2O6P	787.6719	3.3	6.44	SM	22:0	$[M+H]^+$
	C47H89N2O6P	809.6506	-3.7	6.44	SM	24:3	$[M+H]^+$
	C47H93N2O6P	813.6871	2.7	6.54	SM	24:1	$[M+H]^+$
	C49H91N2O6P	835.6672	-2.5	6.54	SM	26:4	$[M+H]^+$
	C48H95N2O6P	827.7049	5.2	6.57	SM	25:1	$[M+H]^+$
	C46H93N2O6P	801.6882	4.1	6.68	SM	23:0	$[M+H]^+$
	C48H91N2O6P	823.6712	2.3	6.7	SM	25:3	$[M+H]^+$
	C47H95N2O6P	815.7028	2.7	6.91	SM	24:0	$[M+H]^+$
	C49H93N2O6P	837.6869	2.4	6.92	SM	26:3	$[M+H]^+$
	C45H89N2O6P	785.6570	4.3	8.38	SM	22:1	$[M+H]^+$
	C49H95N2O6P	839.7038	3.8	8.72	SM	26:2	$[M+H]^+$
	C46H93N2O6P	801.6851	0.2	8.78	SM	23:0	$[M+H]^+$
	C49H97N2O6P	841.7189	3.2	8.9	SM	26:1	$[M+H]^+$
	C53H101N2O6P	893.7510	3.9	8.92	SM	30:3	$[M+H]^+$
	C48H97N2O6P	829.7124	-4.6	8.97	SM	25:0	$[M+H]^+$
	C40H75N2O6P	711.5465	3.4	9.11	SM	17:3	$[M+H]^+$
	C50H99N2O6P	855.7324	0.6	9.21	SM	27:1	$[M+H]^+$
	C52H105N2O6P	885.7817	3.2	9.44	SM	29:0	$[M+H]^+$
	C55H109N2O6P	925.8089	-1.3	9.48	SM	32:1	$[M+H]^+$
TG	C47H89NO6	764.6807	5.1	8.03	TG	44:2	$[M+NH_4]^+$

C49H91NO6	790.6967	5.3	8.11	TG	46:3	$[M+NH_4]^+$
C53H95NO6	842.7266	3.3	8.23	TG	50:5	$[M+NH_4]^+$
C57H99NO6	894.7515	-4	8.23	TG	54:7	$[M+NH_4]^+$
C45H89NO6	740.6752	-2.1	8.24	TG	42:0	$[M+NH_4]^+$
C57H99NO6	894.7515	-4	8.25	TG	54:7	$[M+NH_4]^+$
C50H93NO6	804.7063	-2.2	8.25	TG	47:3	$[M+NH_4]^+$
C55H97NO6	868.7400	0.7	8.3	TG	52:6	$[M+NH_4]^+$
C47H91NO6	766.6937	1.6	8.3	TG	44:1	$[M+NH_4]^+$
C49H93NO6	792.7114	4.2	8.3	TG	46:2	$[M+NH_4]^+$
C61H101NO6	944.7735	3	8.31	TG	58:10	$[M+NH_4]^+$
C51H95NO6	818.7251	1.7	8.33	TG	48:3	$[M+NH_4]^+$
C51H95NO6	818.7239	0.1	8.34	TG	48:3	$[M+NH_4]^+$
C59H101NO6	920.7708	0.1	8.34	TG	56:8	$[M+NH_4]^+$
C46H91NO6	754.6968	5.8	8.36	TG	43:0	$[M+NH_4]^+$
C53H97NO6	844.7397	0.4	8.36	TG	50:4	$[M+NH_4]^+$
C53H97NO6	844.7397	0.4	8.39	TG	50:4	$[M+NH_4]^+$
C57H101NO6	896.7740	3.7	8.41	TG	54:6	$[M+NH_4]^+$
C55H99NO6	870.7558	0.8	8.42	TG	52:5	$[M+NH_4]^+$
C61H103NO6	946.7879	1.6	8.43	TG	58:9	$[M+NH_4]^+$
C50H95NO6	806.7217	-2.5	8.47	TG	47:2	$[M+NH_4]^+$
C52H97NO6	832.7440	5.5	8.49	TG	49:3	$[M+NH_4]^+$
C59H103NO6	922.7908	4.8	8.54	TG	56:7	$[M+NH_4]^+$
C57H101NO6	896.7720	1.5	8.55	TG	54:6	$[M+NH_4]^+$
C49H95NO6	794.7220	-2.2	8.57	TG	46:1	$[M+NH_4]^+$
C53H99NO6	846.7567	2	8.58	TG	50:3	$[M+NH_4]^+$
C51H97NO6	820.7375	-2.3	8.58	TG	48:2	$[M+NH_4]^+$
C55H101NO6	872.7720	1.5	8.62	TG	52:4	$[M+NH_4]^+$
C53H99NO6	846.7554	0.4	8.63	TG	50:3	$[M+NH_4]^+$
C57H103NO6	898.7861	-0.3	8.64	TG	54:5	$[M+NH_4]^+$
C48H95NO6	782.7242	0.6	8.65	TG	45:0	$[M+NH_4]^+$
C52H99NO6	834.7592	5	8.67	TG	49:2	$[M+NH_4]^+$
C54H101NO6	860.7722	1.8	8.7	TG	51:3	$[M+NH_4]^+$
C50H97NO6	808.7390	-0.5	8.7	TG	47:1	$[M+NH_4]^+$
C59H105NO6	924.8026	0.7	8.75	TG	56:6	$[M+NH_4]^+$

C49H97NO6	796.7368	-3.3	8.78	TG	46:0	$[M+NH_4]^+$
C51H99NO6	822.7565	1.8	8.79	TG	48:1	$[M+NH_4]^+$
C53H101NO6	848.7715	1	8.8	TG	50:2	$[M+NH_4]^+$
C55H103NO6	874.7885	2.5	8.82	TG	52:3	$[M+NH_4]^+$
C58H108NO6	916.8366	3.6	8.82	TG	55:3	$[M+NH_4]^+$
C61H115NO6	958.8865	6.5	8.82	TG	58:3	$[M+NH_4]^+$
C57H105NO6	900.8053	3.7	8.83	TG	54:4	$[M+NH_4]^+$
C54H103NO6	862.7913	5.8	8.92	TG	51:2	$[M+NH_4]^+$
C61H109NO6	952.8344	1.2	8.99	TG	58:6	$[M+NH_4]^+$
C51H101NO6	824.7726	2.3	8.99	TG	48:0	$[M+NH_4]^+$
C59H107NO6	926.8182	0.5	9	TG	56:5	$[M+NH_4]^+$
C53H103NO6	850.7871	0.9	9	TG	50:1	$[M+NH_4]^+$
C55H105NO6	876.8063	4.9	9	TG	52:2	$[M+NH_4]^+$
C60H115NO6	946.8836	3.6	9	TG	57:2	$[M+NH_4]^+$
C58H11NO6	918.8494	0.4	9.01	TG	55:2	$[M+NH_4]^+$
C61H117NO6	960.8916	-4.5	9.01	TG	58:2	$[M+NH_4]^+$
C59H109NO6	928.8317	-1.7	9.02	TG	56:4	$[M+NH_4]^+$
C57H107NO6	902.8207	3.4	9.04	TG	54:3	$[M+NH_4]^+$
C51H101NO6	824.7700	-0.8	9.06	TG	48:0	$[M+NH_4]^+$
C54H105NO6	864.8056	4.2	9.07	TG	51:1	$[M+NH_4]^+$
C56H107NO6	890.8201	2.7	9.08	TG	53:2	$[M+NH_4]^+$
C54H105NO6	864.8061	4.8	9.12	TG	51:1	$[M+NH_4]^+$
C59H111NO6	930.8494	0.4	9.21	TG	56:3	$[M+NH_4]^+$
C55H109NO6	880.8375	4.8	9.21	TG	52:0	$[M+NH_4]^+$
C55H107NO6	878.8224	5.4	9.21	TG	52:1	$[M+NH_4]^+$
C54H99NO6	858.7546	-0.6	9.22	TG	51:4	$[M+NH_4]^+$
C57H109NO6	904.8358	2.8	9.22	TG	54:2	$[M+NH_4]^+$
C54H107NO6	866.8201	2.8	9.31	TG	51:0	$[M+NH_4]^+$
C59H113NO6	932.8600	1.4	9.45	TG	56:2	$[M+NH_4]^+$
C57H111NO6	906.8511	2.4	9.46	TG	54:1	$[M+NH_4]^+$
C58H113NO6	920.8690	4.8	9.52	TG	55:1	$[M+NH_4]^+$
C59H115NO6	934.8801	-0.2	9.59	TG	56:1	$[M+NH_4]^+$
C57H113NO6	908.8682	4	9.59	TG	54:0	$[M+NH_4]^+$
C60H117NO6	948.9012	5.6	9.7	TG	57:1	$[M+NH_4]^+$

C61H113NO6	956.8646	2.2	9.8	TG	58:4	$[M+NH_4]^+$
C56H109NO6	892.8337	0.4	9.9	TG	53:1	$[M+NH_4]^+$
C63H121NO6	988.9258	-1.4	9.93	TG	60:2	$[M+NH_4]^+$
C65H123NO6	1014.9415	-1.4	9.93	TG	62:3	$[M+NH_4]^+$
C62H121NO6	976.9298	2.7	9.95	TG	59:1	$[M+NH_4]^+$
C62H123NO6	978.9465	3.7	10.09	TG	59:0	$[M+NH_4]^+$
C65H125NO6	1016.9623	3.7	10.12	TG	62:2	$[M+NH_4]^+$
C63H123NO6	990.9436	0.7	10.12	TG	60:1	$[M+NH_4]^+$

Table S2 in the supplemental information. 10 most abundant* lipid species found in extracted human plasma

Class	Formula	m/z Found	Ppm	Time (min)	Area Abs	provisional assignment
PC	C42H80NO8P	758.5718	2.4	5.02	311	1-acyl 34:2
PC	C44H84NO8P	786.6025	1.6	5.59	210	1-acyl 36:2
PC	C42H82NO8P	760.5883	3.5	5.44	189	1-acyl 34:1
PC	C44H80NO8P	782.5728	3.6	4.94	154	1-acyl 36:4
PC	C44H82NO8P	784.5876	2.5	5.15	134	1-acyl 36:3
TG	C55H103NO6	874.7885	2.5	8.82	109	1-acyl 52:3
TG	C55H105NO6	876.8063	4.9	9	84	1-acyl 52:2
SM	C39H79N2O6P	703.5767	1.9	4.78	60	2-amido 16:0
PC	C46H80NO8P	806.5729	3.7	4.78	58	1-acyl 38:6
TG	C51H99NO6	822.7565	1.8	8.79	15	1-acyl 48:1

* Most abundant as determined by the peak area of the most abundant m/z of each lipid.

Supplemental information Figure S3. High energy fragmentation for the ChoE 18:1 giving rise to the diagnostic fragment-ion at m/z 369.3504 corresponding to the cholesteryl motif which in turn can be used as a precursor ion to 'hunt' in the data set for ChoE lipids in the low energy trace.

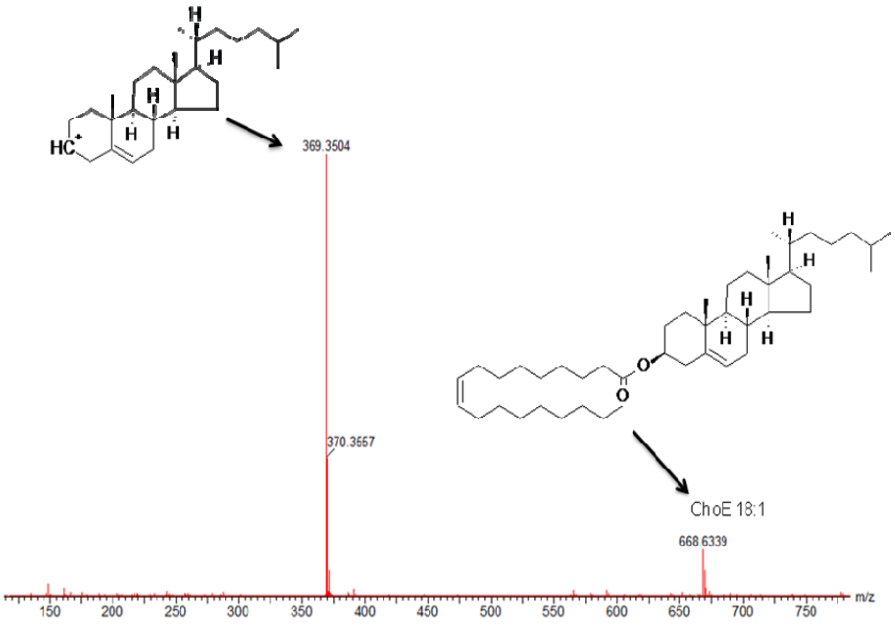

Supplemental information Figure S4. High energy extracted ion precursor ion chromatograms in negative ion mode. In this figure it can be observed (from top to bottom; m/z 303.2332 FA (20:4), m/z 283.2646 FA (18:0), m/z 281.2489 FA (18:1), m/z 279.2332 FA (18:2), m/z 255.2332 FA (16:0), m/z 241.2175 FA (15:0)) the fact that fragment-ion information determining the length of the FA can be search against the low energy mode with exact mass to determine the elemental composition of the lipid and to even quantify the levels present (the low energy data is not shown in this example)

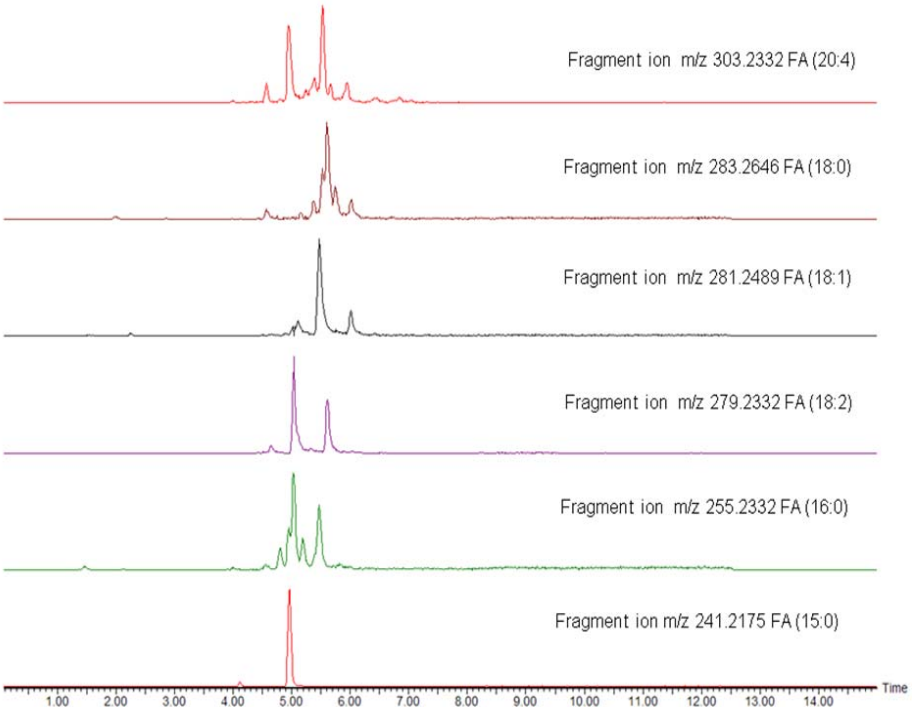

Supplemental information Figure S5. Low energy extracted ion chromatogram of PG 14:0/14:0 with m/z 665.4406 and the corresponding high energy extracted ion chromatogram of m/z 227.2003.